ROLE OF GLYCOSPHINGOLIPIDS IN FORMATION AND FUNCTION OF LIPID RAFTS

MIAO LV

NATIONAL UNIVERSITY OF SINGAPORE
2006

ROLE OF GLYCOSPHINGOLIPIDS IN FORMATION AND FUNCTION OF LIPID RAFTS

BY

MIAO LV
(*B.SC., Wuhan University*)

A THESIS SUBMITTED
FOR THE DEGREE OF MASTER OF SCIENCE

DEPARTMENT OF BIOCHEMISTRY
NATIONAL UNIVERSITY OF SINGAPORE
2006

ACKNOWLEDGEMENTS

I would like to express my heartfelt thanks and respect to my supervisor, Associate Professor, Li Qiutian, Department of Biochemistry, National University of Singapore, for his seasoned guidance, valuable suggestion and discussion, encouragement and patience during my study.

I am indebt to Ms. Tan Boon Kheng for her warm-hearted assistance and unfailing help. I would also like to express my appreciation to my friends, Shao Ke, Zhi Li, Wen Chi, Qing Song and Wei Shi for their help and valuable friendship. They gave me generous support and understanding when I was in the tough time. It is with them that my graduate life became a precious memory. I am also grateful to National University of Singapore for awarding me a research scholarship.

I would like to express my deepest love and gratitude to my parents and family for their dedicated love, support and understanding all the time. Without your support, this thesis wouldn't have been possible.

TABLE OF CONTENTS

Acknowledgments **3**

Table of contents **4**

List of figures **8**

Abbreviations used in text **9**

Summary **11**

CHAPTER 1. INTRODUCTION 14

1.1 Structure of lipid rafts 14

1.1.1. Membrane lipids and phase separation 14

1.1.2. Lipid rafts in Lo phase 15

1.1.3. Lipid interactions in the raft domains 17

1.1.4. Proteins associated with rafts 18

1.2. The GSL 19

1.2.1. The structure and physical properties of GSLs 19

1.2.2. Metabolism of GSLs 21

1.2.2.1. GSL biosynthesis 21

1.2.2.2. GSL degradation 22

1.2.3. NB-DNJ and GSL metabolism 23

1.3. Role of lipid rafts in endocytosis 25

1.3.1. Clathrin-dependent endocytosis and caveolae-dependent endocytosis 25

1.3.2. Lipid rafts and caveolae 26

1.3.3. Markers for caveolae/raft endocytosis 27

1.3.4. Mechanism of caveolae/raft endocytosis 28

1.4. Lipid rafts and NPC disease 30

1.4.1. Cholesterol trafficking in NPC disease 30

1.4.2. NPC and GSL homeostasis 33

1.4.3. Potential role of rafts in cholesterol and GSL homeostasis 34

CHAPTER 2. MATERIALS AND METHODS 36

2.1. Materials 36

2.1.1. Chemicals 36

2.1.2. Media and buffers 39

2.1.2.1. Reagents for cell culture 39

2.1.2.2. Reagents for Western blotting 40

2.1.2.3. Solutions for HPTLC 41

2.1.2.4. Buffer for $DiIC_{18}$ Staining 41

2.1.2.5. Buffer for flow cytometry 41

2.1.3. Instruments and other general consumables 41

2.2. Cell culture 42

2.3. Protein determination 43

2.4. MTT assay 45

2.5. Lipid extraction 46

2.6. HPTLC assay 46

2.7. Isolation of lipid rafts 47

2.8. Western blotting 48

2.9. $DiIC_{18}$ staining 50

2.10. CTxB binding 51

2.11. Flow cytometry 52

2.12. CTxB endocytosis 53

2.13. Filipin staining 54

2.13.1. Effect of progesterone on intracellular trafficking of cholesterol 54

2.13.2. Effect of NB-DNJ on intracellular trafficking of cholesterol in normal cells 55

2.13.3. Effect of NB-DNJ on intracellular trafficking of cholesterol in NPC-like cells 56

CHAPTER 3. RESULTS 58

3.1. Effect of NB-DNJ on GSL biosynthesis in human fibroblast cells 58

3.1.1. Cellular toxicity of NB-DNJ in human fibroblast cells 58

3.1.2. Effect of NB-DNJ on ganglioside biosynthesis in human fibroblast cells 59

3.1.3. Effect of NB-DNJ on cell surface GM1 in human fibroblast cells 61

3.2. Effect of NB-DNJ on raft formation in human fibroblast cells 65

3.2.1. Isolation of lipid rafts from human fibroblast cells 65

3.2.2. Effect of NB-DNJ on raft formation in human fibroblast cells 66

3.3. Effect of NB-DNJ on CTxB endocytosis in human fibroblast cells 69

3.4. Effect of NB-DNJ on intracellular cholesterol trafficking in human fibroblast cells 74

3.4.1. Effect of progesterone on intracellular trafficking of cholesterol in human fibroblast cells 74

3.4.2. Effect of NB-DNJ on intracellular trafficking of cholesterol in human fibroblast cells 76

CHAPTER 4. DISCUSSION 79

4.1. Isolation of lipid rafts 79

4.2. Effect of NB-DNJ on GSL biosynthesis 82

4.3. Effect of NB-DNJ on raft formation 86

4.4. Effect of NB-DNJ on raft-dependent endocytosis 91

4.5. Effect of NB-DNJ on intracellular cholesterol trafficking 98

5. REFERENCE 99

LIST OF FIGURES

Tab.3.1 Cellular toxicity of NB-DNJ in human fibroblast cells. 59

Fig. 3.1 Effect of NB-DNJ on ganglioside biosynthesis in human fibroblast cells. 59

Fig. 3.2 Effect of NB-DNJ on GM3 biosynthesis in human fibroblast cells. 60

Fig. 3.3 The different behaviors of CTxB at 0 ^{o}C and 37 ^{o}C in human fibroblast cells. 62

Fig 3.4 Effect of NB-DNJ on cell surface GM1 in human fibroblast cells. 63

Fig. 3.5 Effect of NB-DNJ on cell surface GM1 in human fibroblast cells. 64

Fig. 3.6 Isolation of lipid rafts from human fibroblast cells. 65

Fig. 3.7 Human fibroblast cells labeled with $DiIC_{18}$. 67

Fig. 3.8 Effect of NB-DNJ on raft formation in human fibroblast cells. 68

Fig. 3.9 Effect of NB-DNJ on CTxB endocytosis in human fibroblast cells. 70

Fig. 3.10 Effect of NB-DNJ on CTxB endocytosis in human fibroblast cells. 71

Fig. 3.11 Effect of NB-DNJ on CTxB endocytosis in human fibroblast cells. 71

Fig. 3.12 Effect of NB-DNJ on CTxB endocytosis in human fibroblast cells. 73

Fig. 3.13 Effect of progesterone on intracellular trafficking of cholesterol in human fibroblast cells. 75

Fig. 3.14 Effect of NB-DNJ on intracellular trafficking of cholesterol in normal human fibroblast cells. 77

Fig. 3.15 Effect of NB-DNJ on intracellular trafficking of cholesterol in NPC-like human fibroblast cells. 78

ABBREVIATIONS USED IN TEXT

BSA	bovine serum albumin
Cer	ceramide
CO_2	carbon dioxide
CTxB	cholera toxin subunit B
$DiIC_{18}$	1, 1'-dioctadecyl-3, 3, 3', 3' tetramethylindocarbocyanine perchlorate
DMEM	Dulbecco's Modified Eagle Medium
DMSO	dimethyl sulfoxide
DPPC	dipalmitoyl phosphatidylcholine
DRM	detergent resistant membrane
EE	early endosome
ER	endoplasmic reticulum
Gal	galactose
Glc	glucose
GM1	Gal_1-3GalNAc_1-4(NeuAc_2-3) Gal_1-4Glc_1-Cer
GM2	GalNAc_1-4(NeuAc_2-3) Gal_1-4Glc_1-Cer
GM3	NeuAc_2-3Gal_1-4Glc_1-Cer
GPI	glycosylphosphatidylinositol
GSL	glycosphingolipid
HPTLC	high performance thin layer chromatography
LacCer	lactosylceramide
LBPA	lysobisphosphatidic acid

Lc	liquid crystalline
L_d	liquid-disordered
LDL	low density lipoprotein
LE	late endosome
Lo	liquid-ordered
LSD	lysosomal storage disorder
LSO	lysosome-like storage organelle
LY	lysosome
MTT	3-(4, 5-dimethylthiazol-2-yl)-2, 5-diphenyltetrazolium bromide
NB-DNJ	N-Butyldeoxynojirimycin
NPC	Niemann-Pick type C
PBS	phosphate-buffered saline
PC	phosphatidylcholines
PE	phosphatidylethanolamine
PFA	paraformaldehyde
PI	propidium iodide
SAT	sialyltransferase
SCAP	SREBP cleavage-activating protein
SDS	sodium dodecyl sulfate
SLSD	sphingolipid storage disease
SM	sphingomyelin
SREBP	sterol regulatory element-binding protein
SV40	simian virus 40

TEMED	N, N, N', N'-tetramethyl-Ethylenediamine
Tm	acyl chain melting temperatures
U18666A	3β-[2-(diethylamino) ethoxy] androst-5-en-17-one

SUMMARY

Recent findings suggest that lipid rafts enriched in glycosphingolipids (GSLs) and cholesterol exist in cell membranes. Raft domains are highly ordered domains characterized by tight acyl-chain packing while other membrane domains are composed by loosely packed phospholipids (Brown and London, 1997). Lipid rafts can be isolated as detergent resistant membranes (DRMs) based on their insolubility in non-ionic detergents such as Triton X-100 at low temperatures (Brown and Rose, 1992). It has been suggested that the head group interactions of GSLs are essential for the formation of functional rafts (Simons and Ikonen, 1997).

To investigate the putative role of GSLs in rafts, specific inhibitor of GSL biosynthesis, N-Butyldeoxynojirimycin (NB-DNJ), was used to manipulate cellular GSL levels of human fibroblast cells. NB-DNJ is known to inhibit the ceramide (Cer) glucosyltransferase which catalyses the first step in GSL biosynthesis, thus results in intense depletion of cellular GSLs (Platt, et al., 1993). The NB-DNJ treated human fibroblast cells were examined by high performance thin layer chromatography (HPTLC) assay for the cellular GSL levels. In addition, the ganglioside GM1 in the plasma membrane was examined by flow cytometry. The results show that in the presence of NB-DNJ, cellular GSLs, in particular GM1, were significantly decreased with NB-DNJ in a dose-dependent manner. The effect of GSL depletion on raft formation was then evaluated by using 1,1'-dioctadecyl-3,3,3',3' tetramethylindocarbocyanine perchlorate ($DiIC_{18}$) staining and confocal microscope. $DiIC_{18}$ is a member of long chain

dialkylcarbocyanines which preferentially partitions into raft domains of the plasma membrane (Sun, et al., 2003), whose fluorescence intensity can then be quantitated by using a quantitative confocal microscopy approach. NB-DNJ depleted cellular GSLs, resulting in the decrease of raft domains in the plasma membrane, indicating that inhibition of GSL biosynthesis does affect raft formation in human fibroblast cells.

Investigation was also carried out to examine the effect of NB-DNJ on raft-dependent endocytosis. Cholera toxin subunit B (CTxB), known to be internalized via raft dependent pathway (Pacuszka and Fishman, 1992), was studied as a marker for raft-dependent endocytosis. GSL depletion led to the inhibition of CTxB endocytosis. Because GSLs may play a role in mediating intracellular trafficking of cholesterol (Marjorie, et al., 2003), in this study, the effect of NB-DNJ on cholesterol intracellular trafficking was also examined, especially in Niemann-Pick type C (NPC) like cells, which are characterized by abnormal accumulation of cholesterol in late endosomes (LE) and lysosomes (LY) (Pentchev, et al., 1995). In both normal cells and NPC like cells, NB-DNJ did not alter the pattern of intracellular cholesterol trafficking, indicating that the removal of GSL alone might not be sufficient to reverse the abnormal intracellular cholesterol trafficking and the interaction of other factors with GSLs might be involved in mediating this process.

CHAPTER 1. INTRODUCTION

1.1. Structure of lipid rafts

1.1.1. Membrane lipids and phase separation

According to the classic fluid-mosaic model of biological membrane, the major lipid component of the membrane bilayer lipids is phospholipid. Phospholipids, along with proteins, cholesterol, and other types of molecules, such as glycosphingolipids (GSLs), form a uniform and homogeneous fluid mixture (Singer and Nicolson, 1972). Because membrane phospholipids are rich in unsaturated acyl chains and have low acyl chain melting temperatures (Tm), cellular membranes are thought to exist in a liquid crystalline (Lc) or liquid-disordered (L_d) phase (Singer and Nicolson, 1972).

However, recent studies suggest that in eukaryotic cells, the plasma membrane and some organelles of the secretory and endocytic pathways are rich in sphingolipids and cholesterol, which may affect dramatically the state of the membrane phases (Silvius, et al., 1996). Spingolipids, including GSLs and sphingomyelin (SM), are unique in having a significantly high Tm. For example, the Tm of SM is about 37-41^{o}C and some GSLs may have Tm of 60-70 ^{o}C. This high Tm is due to the long and largely saturated acyl chains of sphingolipids, which allow them to readily pack tightly together. In addition, the hydrogen bonding between polar headgroups of sphingolipids may also contribute to the tight packing (Brown and London, 1997). In fact sphingolipids tend to form a gel phase

characterized by an ordered and tightly packed structure. In contrast, most phospholipids have Tm below 0 ^{o}C and are loosely packed. They tend to form the Lc phase which is characterized by its lesser order, looser packing and more rapid molecular motion. The differential packing density of sphingolipids and phospholipids may lead to phase separation in the membranes (Brown and London, 2000) and the existence of cholesterol will add complexity to the membrane phases (Silvius, et al., 1996).

The properties of sphingolipids suggest that tightly packed sphingolipids might be separated from the loosely packed phospholipids. In the presence of high amount of cholesterol, sphingolipids tend to form a phase which is more similar to a liquid-ordered (Lo) phase than the gel phase. Lo phase has properties that are intermediate between the gel and Lc phases. Lo phase is characterized by tight acyl-chain packing and extended acyl chains which are similar with the gel phase (Brown and London, 2000). However, unlike the gel phase, acyl chains in the Lo phase have rapid lateral mobility in the bilayer (Almeida, et al., 1992). Lo phase has been identified in binary mixtures of saturated phosphatidylcholines (PC) and cholesterol (Recktenwald and McConnell, 1981; Karlstrom, et al., 1987; Moldovan, et al., 1995; Ipsen, et al., 1987; Vist and Davis, 1990; Mateo, et al., 1995) and requires cholesterol to form. Mixtures of SM and cholesterol also form Lo phase (Sankaram and Thompson, 1990)

1.1.2. Lipid rafts in Lo phase

Recent findings confirmed that GSL- and cholesterol-rich domains do exist in cell membrane. They may exist as Lo phase "rafts" floating in the Lc phase sea (Simons and Toomre, 2000). These domains are named "lipid rafts".

Raft domains can be isolated as detergent resistant membranes (DRMs) based on the insolubility of lipid rafts in non-ionic detergents such as Triton X-100 at low temperatures (Brown and Rose, 1992). It has been known that the GSLs and some of the cholesterol in cell membranes are resistant to extraction by cold detergent while most cellular phospholipids are detergent soluble. DRMs are rich in GSL and cholesterol, suggesting that detergent insoluble Lo phase raft domains may coexist with detergent soluble Lc phase domains in cell membranes (London and Brown, 2000). DRMs are also enriched in a number of proteins. Some of these proteins are targeted to DRMs by linking to saturated acyl chains either in the form of a glycosylphosphatidylinositol (GPI) anchor or through acylation with myristate or palmitate (McConville and Ferguson, 1993). These modifications will help proteins to be accommodated in an ordered environment (Arni, et al., 1998; Zhang, et al., 1998; Melkonian, et al., 1999; Moffett, et al., 2000). The fact that DRMs are present in Lo phase was further supported by observations that Lo phase in the model membrane is resistant to detergent and the DRMs extracted from cells have similar physical properties with model membranes in Lo phase (Ge, et al., 1999). In addition, introduction of detergent-independent methods for visualizing membrane domains and studying their functions provided more support for the Lo phase raft model (Brown and London, 1999; Jacobson and Dietrich, 1999; Janes, et al., 2000). All these evidences

suggested DRMs may be derived from lipid rafts and isolation of DRMs is widely used to study lipid rafts.

It is suggested that rafts may be enriched in plasma membranes, late secretory pathway and endocytic compartments which are enriched in cholesterol and GSLs (Brown and London, 1998). However the intracellular distribution of lipid rafts, especially the behavior of rafts in the inner leaflet of the membrane bilayer, still needs further investigations.

1.1.3. Lipid interactions in the raft domains

Various studies suggested that DRMs' insolubility is due to lipid-lipid interactions. This conclusion is further supported by the model membrane experiments in which detergent insolubility of membranes was observed even in the absence of proteins (Schroeder, et al., 1994). A generally accepted model for the organization of sphingolipid–cholesterol rafts proposes that sphingolipids self-associate through weak interactions between the carbohydrate heads of the GSLs and the interaction of GSLs is essential for raft formation. The GSL headgroups occupy larger areas in the exoplasmic leaflet than their highly saturated lipid hydrocarbon chains do. Cholesterol, with its small headgroup, is recruited to rafts and fills the gaps in the bilayer created by the discrepancy in size between the large GSL headgroups and their acyl chains (Simons and Ikonen, 1997). However this model has been challenged by some recent findings. In a study with model membranes, high-Tm phospholipids, dipalmitoyl phosphatidylcholine (DPPC), was found to be

present in Triton-insoluble DRMs, suggesting that a long, saturated acyl chain structure and a high Tm might be more important for the association of a lipid with raft domains than the structure of its headgroup (Schroeder, et al., 1994). It was also found that DRMs can be isolated from MEB-4 melanoma cell line and its GSL-deficient derivative with similar DRM protein profiles (Ostermeyer, et al., 1999). Thus an alternative model for the structure of rafts has been raised. This model postulates that interactions between lipid acyl chains play a key role in raft formation. Particularly the high Tm of sphingolipids is likely to promote phase separation and formation of raft domains in the presence of high levels of cholesterol (Brown and London, 1998).

1.1.4. Proteins associated with rafts

GPI-anchorage and acylation are the main means for proteins to be associated with rafts. GPI-anchored proteins are the first proteins found in DRMs (Middleton, et al., 1997; Sheets, et al., 1997). GPI-anchored proteins generally contain saturated acyl chains and are thus likely to prefer the association with ordered raft domains (Shenoy-Scaria, et al., 1994). Proteins could also be linked to DRMs by acylation with myristate or palmitate (Pike, 2004). The role of acylation in DRM association has been found in Src family nonreceptor protein tyrosine kinases (Resh, et al., 1994; Milligan, et al., 1995; Robbins, et al., 1995). Modifications by either myristate or palmitate are necessary for the association of these kinases with DRMs (Shenoy-Scaria, et al., 1994; Robbins, et al., 1995). Several other palmitoylated DRM proteins have also been identified (Brown and London, 1997). In these proteins, mutation of the palmitoylation site might block the

DRM association (Maekawa, et al., 1997). Notably, Caveolin, a marker of rafts might be an exception. Elimination of its three palmitoylation sites does not affect its association with DRMs (Dietzen, et al., 1995).

DRMs are relatively poor in transmembrane proteins and prenylated proteins (Fujimoto, 1996). This might be due to the fact that membrane-spanning proteins and prenyl groups are difficult to be accommodated in the highly ordered environment of lipid rafts. However, there are several specific transmembrane proteins which are found in DRMs. The mechanism of how these proteins associate with DRMs is poorly understood. The amino acid sequence of the membrane-spanning domain may affect DRM localization (Perschl, et al., 1995; Scheiffele, et al., 1997; Field, et al., 1999), and might be important for the protein lipid interactions. However, mutations in the cytoplasmic domains that are unlikely to directly interact with lipids can also affect the association with DRMs (Puertollano, et al., 1998; Polyak, et al., 1998; Bruckner, et al., 1999; Machleidt, et al., 2000).

1.2. The GSL

1.2.1. The structure and physical properties of GSL

GSLs consist of a hydrophobic ceramide (Cer) backbone and a polar sugar headgroup. The Cer part contains a sphingoid base and a fatty acid. The different combinations of different headgroups, sphingoid bases and fatty acyl chains create various structures of

GSLs. The sphingoid bases can vary in length, saturation level, hydroxylation and branching (Karlsson, 1970). The fatty acid is amide-linked to the amino group of the sphingoid base and can also vary in length, saturation and hydroxylation. In mammalian cells, the GSLs carry saccharide moiety on the Cer backbone. In mammals, the two main classes of GSLs contain either galactose (Gal) or glucose (Glc) as the first saccharide moiety. The saccharide moiety of GSLs could be a single saccharide unit, as in the case of cerebrosides (Glc-Cer and Gal-Cer), or sulphated mono- or disaccharides (sulphatides), or a linear or branched oligosaccharide chain where Gal, Glc, nacetylglucosamine, N-acetylgalactosamine, fucose, sialic acid, and glucuronic acid are the possible components .The mono- or multi-sialosylated GSLs constitute the family of gangliosides. Some gangliosides are also sulphated (Tadano-Aritomi, et al., 1998).

In mammalian cells GSLs have two striking structural features. Firstly, the fatty acid species are mostly long and saturated (Rosenthal, 1987). Secondly, the region between the headgroup and the backbone contains chemical groups that can function both as hydrogen bond donor and acceptor. Additional hydrogen bonding can therefore occur between the sugar headgroups of GSLs (Pascher, 1976). In cell membranes, the Cer part is inserted in the cellular membrane while the sugar headgroup commonly faces the non-cytosolic space (Tettamanti, 2004).

1.2.2. Metabolism of GSL

1.2.2.1. GSL biosynthesis

The biosynthesis of GSLs takes place on intracellular membranes including endoplasmic reticulum (ER) and Golgi apparatus and is catalysed by membrane-bound enzymes. GSL de novo biosynthesis starts with the formation of Cer. This step is catalyzed by membrane bound enzymes at the cytosolic leaflet of the ER (Mandon, et al., 1999). The 4-trans double bond of the sphingoid base is introduced after acylation of sphinganine. The next steps of GSL formation happen in the Golgi apparatus and involve stepwise glycosylation of Cer (Keenan, et al., 1974; Pacuszka, et al., 1978). For example, The Glc is transferred to Cer to form glucosylceramide (Glc-Cer). Transport of Cer from the ER to the Golgi is through both vesicular membrane flow (Van Meer, 1989) and non-vesicular transport (Lipsky and Pagano, 1985; Pagano and Sleight, 1985). The enzymes catalyzing the first two glycosylation steps, including glucosyltransferase and galactosyltransferase I, are found at the cytosolic side of the Golgi (Trinchera, et al., 1991). However the precise localization of Cer glucosyltransferase is still not established. Several groups have reported that it could be on the Golgi and/or a pre Golgi compartment (Coste, et al., 1986; Fukikan and Pagano, 1991; Jeckel, et al., 1992)

For ganglioside biosynthesis, monosaccharide and sialic acid residues are introduced to the growing oligosaccharide chain, yielding series of gangliosides. Firstly, Glc-Cer is glycosylated to form Lac-Cer which is catalysed by Lac-Cer synthase (Carey and

Hirschberg, 1981; Yusuf, et al., 1983). Lac-Cer is then sialosylated to GM3, GM3 to GD3, GD3 to GT3, by the action of three sialyltransferases (SAT I, SAT II and SAT III). Each of these enzymes recognizes specifically the acceptor substrate. GM3, GD3 and GT3, are the starting points for the a-series, b-series and c-series gangliosides respectively. Along each series, non specific N-acetyl-galactosaminyltransferase, galactosyl-transferase and sialyltransferase (SAT IV) introduce a residue of N-acetylgalactosamine, galactose, and sialic acid subsequently, yielding more complex gangliosides (Huwiler, et al., 2000). Enzymes involved in these stepwise reactions are located at the luminal face of the Golgi membranes (Carey and Hirschberg, 1981) and only a small number of glycosyltransferases are involved in the further elongation of the oligosaccharide chains (Sophie, et al., 2004).

1.2.2.2. GSL degradation

GSLs are degraded along the endocytotic route in the late endosomes (LEs) and lysosomes (LYs) by the action of hydrolytic enzymes. This process is assisted by activator proteins and negatively charged lipids (Keenan, et al., 1974; Yusuf, et al., 1983). GSLs are sequentially hydrolyzed from the non-reducing end by specific hydrolases. Defects in the degradation of GSLs (either in glycosidases or their activator proteins) result in GSL storage in the LY. Lysosomal storage disorders (LSDs) are caused by the defective activity of different lysosomal enzymes and integral membrane proteins which results in accumulation of undegraded metabolites in the LY. It is estimated that there are at least 50–60 soluble hydrolases (Journet, et al., 2002) and at least 11 integral membrane

proteins (Eskelinen, et al., 2003) in the LY. Mutations in the genes that encode any of these proteins could cause LSD. These mutations include missense, nonsense and splice-site mutations, partial deletions and insertions. Some mutations lead to the complete loss of enzyme activity while others lead to reduced activity. LSDs normally involve only one single gene, however, for most LSDs, numerous mutations have been described in the same gene in different patients (Futerman and van Meer, 2004).

Over 40 LSDs that involve soluble hydrolases are known. For example, Sphingolipidoses, a subgroup of LSDs, are defined as disorders caused by a defect in enzymes or activator proteins which are responsible for catabolism of sphingosine-containing lipids. LSDs could also be grouped by the accumulated substrate. For example, diseases in which sphingolipid are accumulated could be defined as sphingolipid storage diseases (SLSDs) (Futerman and Van Meer, 2004). Among the LSDs, Niemann-Pick type C (NPC) disease is of particular interest and it will be discussed in details in Section 1.4.

1.2.4. NB-DNJ and GSL metabolism

The imino sugar N-Butyldeoxynojirimycin (NB-DNJ) is an analogue of glucose. It inhibits the Cer glucosyltransferase which catalyses the first step in GSL biosynthesis. This results in extensive GSL depletion (Platt et al., 1993). NB-DNJ causes GSL depletion in many cell lines. For example, it was observed that 90% inhibition of GSL biosynthesis was achieved by treatment with NB-DNJ in HL-60 cells (Platt, et al., 1994). The effect of NB-DNJ on GSL biosynthesis has also been investigated *in vivo*. One group

reported that long term administration of NB-DNJ caused 50-70% GSL reduction in all tissues examined in young mice. Although NB-DNJ is also a potent inhibitor of other enzymes, including α-glucosidase I and II, which could potentially cause side effects both *in vitro* and *in vivo*, results showed that NB-DNJ has little toxic effect in vitro and the administration of NB-DNJ was well tolerated in mice (Platt, et al., 1997).

The mechanism of how NB-DNJ inhibits GSL biosynthesis is not fully understood. It is suggested that alkylation plays a key role in this mechanism since the deoxynojirimycin does not exhibit any inhibition activity (Platt, et al., 1994). However it is not clear whether the alkylation is important for direct enzyme inhibition or for targeting the compound to the membranes where the glucosyltransferase is active (Coste and Martel, 1985).

NB-DNJ, as a specific inhibitor of GSL biosynthesis, provides a convenient approach for manipulating cellular GSL level. One advantage of this approach is that it becomes possible to investigate the effects of partial depletion of GSLs. In addition, NB-DNJ has the potential to be used for the treatment of the GSL lysosomal storage diseases (Platt, et al., 1994).

1.3. Role of lipid rafts in endocytosis

Rafts are dynamic regions serving as a platform for various functions in cell membranes. Both proteins and lipids can move in and out of raft domains with different kinetics. Rafts are most abundant in plasma membrane thus may play an important role in membrane trafficking and signaling. Rafts may also function in secretory and endocytic pathway. However, the exact functions of rafts are still debatable. This is mainly due to the fact that raft domains are too small to be optically resolved (Lawrence and Simons, 2005). In this section the role of rafts in endocytosis will be discussed. The potential role of rafts in maintaining cholesterol and GSL homeostasis will be discussed in the following sections.

1.3.1. Clathrin-dependent endocytosis and caveolae-dependent endocytosis

Up to today the best-characterized endocytosis pathway is the one mediated by clathrin-coated pits. Clathrin-dependent internalization of many molecules has been described in molecular details (Roy and Wrana, 2005). However It was found that certain molecules were internalized continuously with the mutation of some proteins necessary for functional clathrin-coated pits, such as dynamin (Bliek, et al., 1993), eps15 (Benmerah, et al., 1999), epsin (Chen, et al., 1998) and AP180 (Ford, et al., 2001). These findings suggested that there are alternative endocytosis pathway(s) other than the pathway mediated by clathrin-coated pits. Recent research has demonstrated the existence of such pathways (Roy and Wrana, 2005), among which the endocytosis through caveolae is of particular interest. Caveolar endocytosis pathway mediate the internalization of sphingolipids and sphingolipid binding toxins, such as cholera toxin subunit B (CTxB), GPI-anchored proteins, endothelin, growth hormone, IL2 receptors, viruses and bacteria

(Nichols and Lippincott, 2001; Duncan, et al., 2002; Johannes and Lamaze, 2002; Pelkmans and Helenius, 2002; Conner and Schmid, 2003). Caveolae are 50-70nm flask-shaped invagination in the plasma membrane. Caveolin, A 22-kDa protein, is often associated with caveolae and may play an important role in caveolae formation (Brown and London, 1998). However, it should be pointed out that caveolar function is not equal with that of caveolins. It is suggest that caveolin 1 is not necessary for clathrin-independent endocytosis since cholesterol-sensitive, clathrin-independent endocytosis occurs in cell types that naturally lack caveolin 1 but abundant in caveolae structures (Orlandi and Fishman, 1998; Lamaze, et al., 2001).

1.3.2. Lipid rafts and caveolae

Evidences have arisen that lipid rafts may play an important role in caveolar endocytosis. Firstly, almost all molecules known to be internalized by clathrin-independent pathway are found to be enriched in DRMs while molecules taken up by clathrin-dependent pathway are not (Nichols and Lippincott-Schwartz, 2001). This suggests that raft components might be internalized by caveolar endocytosis and excluded from the clathrin-dependent pathway. Secondly, it was found that depletion of cholesterol led to blocking of endocytosis of many molecules. Presumably the decrease of functional rafts may account for the block of endocytosis (Simons and Ikonen, 1997; Edidin, 2003).

There are other evidences that strengthened the link between lipid rafts and caveolae. It has been shown that DRM markers such as GPI-anchored proteins and GSLs accumulate

in caveolae (Brown and London, 1998). GM1 is concentrated in caveolae when detected with CTxB (Tran, et al., 1987; Parton, 1994). Several neutral GSLs and GPI-anchored proteins have also been found in caveolae (Fujimoto, 1996). Moreover, cholesterol is suggested to be enriched in caveolae (Smart, et al., 1996) where caveolin 1 binds to cholesterol. As a result, it becomes unusually resistant to detergent extraction (Sargiacomo, et al., 1993; Murata, et al., 1995). All these findings suggest that caveolae constitute a type of lipid rafts (Harder and Simons, 1997). It is proposed that DRMs exist in cells as rafts within caveolae although rafts may not be restricted to caveolae (Brown and London, 1998). It is suggested that caveolae and rafts mediate a common endocytic pathway, caveolae/raft-dependent endocytosis, defined by its clathrin independence, dynamin dependence, sensitivity to cholesterol depletion, and the morphology and lipid composition of the vesicular intermediate (Nabi and Le, 2003).

1.3.3. Markers for caveolae/raft endocytosis

Many cells including adipocytes and fibroblasts are abundant in caveolae and an endocytic role for caveolae has been well described (Parton and Richards, 2003). For example, it has been shown that GPI-anchored proteins are translocated to caveolae and subsequently internalized (Upla, et al., 2004; Sato, et al., 2004). Some non-enveloped viruses, such as simian virus 40 (SV40), enter cells via caveolae and then are delivered to caveosomes (Pelkmans and Helenius, 2002). CTxB has also been found be internalised via caveolae/raft endocytic pathway (Pelkmans and Helenius, 2002). Cholera toxin belongs to a family of structurally homologous hexameric AB_5 bacterial toxins (Lindberg,

et al., 1987). These toxins consist of an enzymatically active A subunit and a binding B binding subunits (Ling, et al., 1998). CTxB binds the ganglioside GM1 at the cell surface and hence associates with lipid rafts (Spangler, 1992). After internalization, CTxB can be found in early and recycling endosomes, the Golgi apparatus and the ER (Richards, et al., 2002; Majoul, et al., 1996; Majoul, et al., 1998). Notably SV40 and CTxB are delivered by different populations of caveolin-1–positive endocytic compartment (Nichols, 2002), indicating that these two caveolar ligands are sorted to distinct endosomal populations before the delivery to the Golgi and ER. It is also observed that CTxB and SV40 could have significantly different resident times in the Golgi even when they take the same retrograde route to the ER. It is also possible that sorting of SV40 and CTxB may take place either at the plasma membrane, targeting different caveosome populations, or via segregation within the caveosome. All of these sorting mechanisms may lead to different intracellular targeting routes (Nabi and Le, 2003). CTxB has been extensively used as a caveolae/raft endocytosis marker and the analysis of the toxin entry pathway is providing new evidence into caveolae/raft endocytosis pathway.

1.3.4. Mechanism of caveolae/raft endocytosis

The mechanism of caveolae/raft endocytosis is still under investigation. Apparently, CTxB is internalized by caveolae budding (Montesano, et al., 1982; Tran, et al., 1987). It was reported that the phosphatase inhibitor, okadaic acid, caused caveolae budding and the internalization of associated proteins (Parton, et al., 2003). It was proposed that the internalization of caveolae was regulated by phosphorylation and involved the actin

cytoskeleton. Consistent result was reported in the observation of SV40 entry. SV40 infection activated a tyrosine kinase signaling pathway and resulted in recruitment of both dynamin and cortical actin to the virus binding sites. These molecules were suggested to mediate budding of virus-containing caveolae into the cells (Pelkmans, et al., 2002).

The role of caveolin 1 in caveolae/raft endocytosis also remains debatable. As stated above, it has been suggested that caveolar function is not equal with that of caveolin (Orlandi and Fishman, 1998; Lamaze, et al., 2001). Furthermore, experiments based on overexpression of caveolin 1 suggested that caveolin 1 down-regulates caveolar budding (Minshall, et al., 2000). The uptake of CTxB was also decreased by overexpression of caveolin 1 (Nabi and Le, 2003), while decreased expression of caveolin 1 in NIH-3T3 cells increased clathrin-independent uptake of autocrine motility factor. This effect was reversed when caveolin 1 expression was artificially increased (Nabi and Le, 2003). These findings led to the hypothesis that there are caveolae which do not contain caveolin 1 and caveolae which contain caveolin 1. Caveolin 1-negative caveolae exist as transient intermediates during budding into the cells and these intermediates are stabilized by caveolin 1, thus slowing the rate of budding (Nabi and Le, 2003). However, this area still needs further investigation and discovery of new proteins required for caveolar endocytosis are expected.

1.4. Lipid rafts and NPC disease

1.4.1. Cholesterol trafficking in NPC disease

NPC is an early childhood disease exhibiting enlarged liver and spleen as well as progressive neurological degeneration. At the cellular level, the disease is a result of cholesterol accumulation in certain endocytic organelles, which have been characterized as the LE and LY (Pentchev, et al., 1995). These organelles are named lysosome-like storage organelles (LSOs).

The link between NPC and cholesterol was initially reported by Pentchev (Pentchev, et al., 1985). In the following years, characterization of the NPC defect was mostly carried out in patient fibroblasts although similar NPC defect was reported in CHO cells (Neufeld, et al., 1999; Liscum and Faust, 1989; Cruz, et al., 2000). In all these cases, cholesterol accumulation in the LE / LY was observed. Thus NPC has been primarily described as a defect in intracellular cholesterol trafficking. In normal cells, exogenous cholesterol is internalized in the form of low density lipoprotein (LDL) and transported to sorting endosomes. From there, it can be recycled to the plasma membrane or transported to the LE / LY. Cholesterol esters in LDL are hydrolyzed before being released from the LE / LY and free cholesterol is continuously cycled to the plasma membrane and transported to the ER (Cruz, et al., 2000; Lange, et al., 2000). ER serves as a control centre for cholesterol homeostasis and this control system involves membrane-bound transcription factors called sterol regulatory element-binding proteins (SREBPs) which cycle between the ER and the Golgi (Brown and Goldstein, 1997) In sterol-depleted cells the SREBP N-terminus is released from the membrane by proteolysis and enters the

nucleus to activate transcription of genes for the cholesterol and fatty acid biosynthetic pathways and the LDL receptor. Cleavage of SREBP requires two ER proteases and SREBP cleavage-activating protein (SCAP) (Sakai, et al., 1998; Zelenski, et al., 1999; Hua, et al., 1996). When the cellular cholesterol level increases, SREBP proteolysis is abolished, which limits the further synthesis of cholesterol by suppressing transcription of sterol-synthesizing genes, such as 3-hydroxy-3-methylglutaryl-CoA reductase. Cholesterol arriving in the ER membrane also activates and serves as substrate for an ER enzyme, acyl CoA:cholesterol acyltransferase, which catalyzes the esterification of a fatty acid to cholesterol for storage in cytosolic lipid droplets (Chang, et al., 1997; Chang, et al., 1998). Thus, the cellular-free cholesterol levels are precisely controlled.

In NPC cells, cholesterol uptake, delivery to the LE / LY, and cholesterol ester hydrolysis are normal. However, compared with the normal cells, cholesterol accumulates in the LE / LY in large amounts. This cholesterol accumulation could be detected by filipin staining, indicating that the cholesterol is free, or unesterified cholesterol. As a result, the increasing level of cholesterol in the cell is not sensed by the ER and the homeostatic mechanisms are not activated. The LE / LY continue to accumulate cholesterol and change morphologically to become highly enlarged LSOs (Pentchev, et al., 1995; Liscum, et al., 1998). It was reported that mutations of the gene encoding NPC1 and NPC2 can be the causes of NPC disease, among which npc1 mutation is the major type (Carstea, et al., 1997; Loftus, et al., 1997; Liscum, 2000), while 5% is due to defect of npc2 defective. NPC1 protein is a multi-spanning membrane protein with several interesting domains

(Ioannou, 2000; Ioannou, 2001). However the precise function of NPC1 protein is still unknown.

Interestingly, several steroids, including U18666A (hydrophobic amines) and progesterone (non-amines) have been reported to induce extensive cholesterol accumulation in the LE / LY in normal cells. It was reported that progesterone strongly blocked cholesteryl ester synthesis and the steroid induced sequestration of cholesterol in the LE / LY appeared to represent a structurally specific effect. In addition, the progesterone-induced cholesterol accumulation is readily reversible through steroid washout (Butler, et al., 1992). Cytochemically the intracellular accumulation of cholesterol in progesterone-treated cells is indistinguishable from the cholesterol accumulation in the LE / LY in NPC cells (Blanchette-Mackie, et al., 1988). The exact relationship between the NPC defect and the steroid-induced cholesterol accumulation remains unknown. It is suggested that hydrophobic compounds might function by binding to lysobisphosphatidic acid (LBPA), which might play a role in mediating the dynamic flow between internal vesicles and the outer membrane in the LE in normal cells. The hydrophobic amines might interfere with this process, thus affecting the composition of these membranes and the localization of NPC1 protein (Liscum, 2000). Progesterone, which induces inhibition and restoration of the LE / LY cholesterol trafficking has been extensively used as an experimental means to study intracellular cholesterol trafficking.

1.4.2. NPC and GSL homeostasis

As described above, NPC has been primarily described as a defect in intracellular cholesterol trafficking. It was reported that in the neurons of NPC patients, GSLs such as GM2 accumulated in the LE / LY while only negligible increase of cholesterol level was observed (March, et al., 1997). It was also reported that level of GSLs, including GM2, was increased in NPC fibroblasts (Yano, et al., 1996). Thus NPC disease is not only a cholesterol storage disease but also a sphingolipid storage disease. Furthermore, it was reported that mice neurons which are deficient in both NPC1 and the GSL synthesis enzyme exhibited both lack of GM2 accumulation and dramatic reduction in free cholesterol. Thus the cholesterol accumulation in NPC1 deficient neurons appeared to be ganglioside dependent (Marjorie, et al., 2003). It is suggested there is a link between the cholesterol and GSL homeostasis.

The link between NPC disease and the GSL homeostasis was also implied in the report from Pagano's group (Watanabe, et al., 1998). They used BODIPY-lactosylceramide (LacCer) and several other sphingolipids (SM, Gal-Cer, GM1) to trace lipid movement in normal human fibroblasts and fibroblasts from different SLSDs. In normal human fibroblasts, BODIPY-LacCer was internalized and then transported from plasma membrane to the Golgi complex. In SLSD fibroblasts, as expected, BODIPY-LacCer accumulated in the LE / LY. Surprisingly, cholesterol was also found to accumulate in the LE / LY in SLSD fibroblasts. Furthermore, when the SLSD fibroblasts were cultured in LDL-deficient medium, the BODIPY-LacCer did not accumulate in the LY but instead went to the Golgi. Consistently, when the normal fibroblasts were cultured with excess LDL-cholesterol, BODIPY-LacCer was observed to accumulate in the LY. Similar

accumulation of BODIPY-LacCer was also observed in NPC1 fibroblasts. All these data suggested that the cholesterol homeostasis was perturbed in multiple SLSDs secondary to sphingolipid accumulation, and cholesterol played a major role in regulating the traffic of sphingolipids along the endocytic pathway.

1.4.3. Potential role of rafts in cholesterol and GSL homeostasis

Why does LSD cause cholesterol accumulation and how does cholesterol regulate the sphingolipid trafficking? The answer to these questions remains unknown. Simons and Gruenberg (Simons and Gruenberg, 2000) proposed a model, in which lipid rafts in the endocytic pathway might play a role in the regulation of rafts lipids trafficking. They suggested that degradation of sphingolipids is normal when cholesterol is exiting normally from the LE. Similarly, cholesterol removal from the LE would operate normally only when amount of sphingolipids in the LE is low. In lipid storage diseases involving raft lipids, the accumulation of one class of raft lipids would slowly lead to trapping of other raft lipids in the LE. Deregulated accumulation of either raft lipid would then jam both sphingolipid degradation and cholesterol trafficking. Raft lipid accumulation in the LE / LY is also likely to lead to a traffic jam affecting the distribution of other lipids and proteins. This model suggested some possible mechanisms by which lipid rafts may regulate lipid trafficking in endocytic pathways. First, mistargeting of raft components in lipid storage disorders might cause some proteins, which would normally be associated with rafts in the peripheral plasma membrane or early endosome (EE) to be redistributed to the LE / LY. Recent studies indicate that

annexin II is redistributed from its normal localization in the EE and the plasma membrane, to the LE in NPC cells. Second, raft lipid accumulation is expected to alter the properties of the LE / LY membranes, including LBPA-rich membranes, so that they start to form the LY containing lipid lamellae characteristic of lipid storage diseases. This trapping could be caused by the affinitive association of sphingolipids with cholesterol, which is the driving force for raft assembly. Raft accumulation might flatten the highly curved internal membranes within the LE and transform the internal membranes into lamellae. This accumulation and the resulting transformation would interfere with the normal sorting and trafficking capacity of this organelle, as appears to be the case in NPC fibroblasts (Kobayashi, et al., 1999).

The objective of this project is to investigate the effect of GSL depletion on raft formation and function in human fibroblast cells. NB-DNJ will be employed to manipulate the cellular GSL levels in human fibroblast cells. The raft formation will be examined by confocal microscope after the GSL depletion. The effect of GSL depletion on raft-dependent endocytosis will be investigated by using CTxB as a marker. The effect of GSL depletion on intracellular cholesterol trafficking will also be examined by filipin staining.

CHAPTER 2. MATERIALS AND METHODS

2.1. Materials

2.1.1. Chemicals

The following reagents were purchased from BioRad (Hercules, CA, USA)

Prestained broad range precision protein standards, ammonium persulfate, acrylamide/bis solution, bromophenol blue, RC DC protein assay kit (including DC protein assay reagent A, DC protein assay reagent B, DC protein assay Reagent S, RC protein assay reagent I, RC protein assay reagent II)

The following reagent was purchased from BD (San Jose, CA, USA)

Anti flotillin-1 mouse monoclonal IgG1

The following reagent was purchased from Calbiochem (San Diego, CA, USA)

Fluor save^{TM} reagent, low-density lipoprotein (LDL), N-Butyldeoxynojirimycin (NB-DNJ)

The following reagent was purchased from Cambrex (East Rutherford, NJ, USA)

Dulbecco's Modified Eagle Medium (DMEM)

The following reagent was purchased from Duchefa Biochemie (Haarlem, Nethelands)

Polysorbate 20 (TWEEN 20)

The following reagent was purchased from Hayman Limited (Eastways Park, England)

Ethyl alcohol

The following reagent was purchased from HyClone (Logan, UT, USA)

Fetal bovine serum

The following reagents were purchased from Invitrogen (**Carlsbad, CA, USA)**

Glutamine, penicillin-streptomycin

The following reagents were purchased from J. T. Baker (Phillipsburg, NJ, USA)

Tris (Base)

The following reagents were purchased from Merck (Darmstadt, Germany)

Chloroform, methanol, Triton X-100, glycin, acetic acid, isopropanol, 25 TLC aluminum sheets 20×20cm silica gel 60

The following reagents were purchased from Molecular Probes (Eugene, OR, USA)

Cholera toxin subunit B (CTxB) Alexa Fluor 488 conjugate, cholera toxin subunit B (CtxB) Alexa Fluor 594 conjugate, 1,1'-dioctadecyl-3,3,3',3' tetramethylindocarbocyanine perchlorate ($DiIC_{18}$)

The following item was purchased from Pall (East Hills, NY, USA)

Bio Trace™ PVDF (polyvinglidene fluoride) transfer membrane

The following reagents were purchased from Pierce (Rockford, IL, USA)

Super signal west femto maximum sensitivity substrate, super signal west pico chemiluminescent substrate, bond-breaker™ TCEP solution, 8×10 inches clear blue X-Ray film

The following reagent was purchased from Roche Diagnostics (Basel, Switzerland)

Complete EDTA-free protease inhibitor cocktail tablets

The following reagents were purchased from Santa Cruz Biotechnology (Santa Cruz, CA, USA)

Anti caveolin-1 rabbit polyclonal IgG

The following reagents were purchased from Sigma-Aldrich (St. Louis, MO, USA)

Trypsin-EDTA solution, dimethyl sulfoxide (DMSO), filipin complex, Gal_1-3GalNAc_1-4(NeuAc_2-3)Gal_1-4Glc_1-Cer (GM1), GalNAc_1-4(NeuAc_2-3)Gal_1-4Glc_1-Cer (GM2), NeuAc_2-3Gal_1-4Glc_1-Cer (GM3), N,N,N',N'-tetramethyl-

ethylenediamine (TEMED), 3-(4,5-dimethylthiazol-2-yl)-2,5-diphenyltetrazolium bromide (MTT), orcinol, paraformaldehyde (PFA), propidium iodide (PI), progesterone

The following reagent was purchased from Soxal (Singapore)

Carbon dioxide (CO_2), pure liquid nitrogen

2.1.2. Media and buffers

2.1.2.1. Reagents for cell culture

Complete DMEM medium

Dulbecco's Modified Eagle Medium supplemented with 15% (v/v) heat inactivated fetal bovine serum and a mixture of L-glutamine (2mM, final concentration, the same below), penicillin (100unit/ml) and streptomycin (100μg/ml)

Frozen medium

Dulbecco's Modified Eagle Medium supplemented with 40% (v/v) heat inactivated fetal bovine serum with 10% DMSO

Lysis buffer

50 mM Tris-HCl, pH7.5, 150 mM NaCl, 1mM EDTA, 1% Triton-X-100

PBS

1.76 mM KH_2PO_4, 10 mM Na_2HPO_4, 137 mM NaCl, 9 mM KCl, pH7.4

Trypsin-EDTA

0.05% trypsin and 0.02%EDTA

2.1.2.2. Reagents for Western Blotting

4×Resolving gel buffer

1.5 M Tris-HCl, pH 8.8

4×Stacking gel buffer

0.5 M Tris-HCl, pH6.8

5×Loading buffer

1 g SDS, 5 g sucrose, 0.01 g bromophenol blue, 3.125 ml 1M Tris-HCl (pH6.8), 1 ml TCEP, 3 ml distilled water, mixed well by stirring overnight

10×Transfer buffer

30.3 g Tris and 144.13 g glycine in 1 liter distilled water.

Blocking buffer

5% Anlene skimmed milk in TBS

5×Running buffer

15.15 g Tris-HCl, 72 g glycine and 5 g SDS in 1 liter distilled water

TBS

6.075 g Tris and 8.766 g NaCl dissolved in 1 liter distilled water, pH adjusted to 7.5

TBST

0.1% TWEEN 20 in TBS buffer

Transfer buffer

100 ml 10×transfer buffer topped up to 800 ml with distilled water, mixed well, then 200 ml methanol added

2.1.2.3. Solutions for HPTLC

Developing Solvent

Chloroform /methanol /0.2%$CaCl_2$ in water (65:25:4, v/v/v)

Orcinol-H_2SO_4 Reagent

0.2 g orcinol in 100ml 1.5N H_2SO_4

2.1.2.4. Buffer for $DiIC_{18}$ Staining

Medium 1

150 mM NaCl, 5 mM KCl, 1 mM $CaCl_2$, 1 mM $MgCl_2$, and 20 mM Hepes, pH 7.4; supplemented with 2 g/liter glucose

2.1.2.5. Buffer for flow cytometry

Buffer A

2% BSA and 0.1% Na3N in PBS

2.1.3. Instruments and other general consumables

The instruments and general consumables used in this work include: Biological Safety Cabinet Class II (Ann Arbor, MI, USA), Beckman Coulter flow cytometer (Epics Altra)

(Beckman Coulter, Fullerton, CA, USA), Beckman X100 ultracentrifuge (Beckman Coulter, Fullerton, CA, USA), CO_2 Incubator (Heraeus Kulzer, Chatswood, Australia), Camag Nanomat 4 TLC sampler (Camag Scientific Inc., Wilmington, NC,USA) Eppendorf Centrifuge 5810R (B. BRAUN, Melsungen, Germany), pH meter (Beckman Coulter, Fullerton, CA, USA), OLYMPUS IX71 Fluorescence Microscope and Olympus FLVOVIEW 500 inverted microscope (Olympus Technologies, Tokyo, Japan), Orbital Shaker 100 (ARMALAB, Bethesda, MD, USA), Water Bath (MEMMERT**,** Schwabach, Germany), PowerPac Basic Power Supply 100 (Bio-Rad Laboratories, Hercules, CA, USA), Vortex machine (VWR Scientific, West Chester, PA, USA), Ultrasonic Water Bath (ITS Science and Medical, Singapore), Blue MAXTM Polypropylene Conical Tube, Nonpyrogenic serological pipet (Singapore), MULTIDISH 6-wells, 12-wells, 48-wells, 96-wells and Easy Flask (NUNC, Roskilde, Denmark).

2.2. Cell culture

The human fibroblast cells (GM00730A) were obtained from NIGMS Human Genetic Cell Repository, Coriell Institute for Medical Research and maintained in complete DMEM medium at 37°C in a humidified atmosphere containing 5% CO_2.

To initiate a new flask

1) The complete DMEM medium was pre-warmed at 37°C before use. The pipettes and culture flasks were irradiated with ultraviolet rays for 30 min in the culture hood.

2) The cells were removed from liquid nitrogen tank and thawed at 37°C in water bath immediately. Then cells were rapidly transferred into a 25-cm^2 flask. Another 5ml warm complete DMEM medium was added into the flask. The flask was placed in HERA CO_2 incubator at 37°C in a humidified atmosphere containing 5% CO_2 overnight.
3) The cells were washed with warm PBS and the medium in the flask was replaced by fresh complete DMEM medium on the next day.
4) The cells were passaged after 4-5 days when the cells reached about 80%-90% confluence.

Cell passage

1) The cells were washed with warm PBS buffer once.
2) Two ml trypsin-EDTA was added to a 75-cm^2 flask for 3 min. Beat the flask gently to dislodge the cells.
3) The action of trypsin was terminated with 6 ml complete DMEM medium. The cells were resuspended in an appropriate volume and then transferred to a new flask. 15 ml of complete DMEM medium was subsequently added into one flask.

Cells frozen

The subconfluent cells were trypsinised and centrifuged at 400 ×g for 5 min at room temperature. The cell pellet was resuspended in 1 ml frozen medium and stored in NUNC Cryo Tube vials. The tubes were kept at 4°C for half an hour, then at -20°C for 2 hour,

subsequently at -80°C overnight before being transferred into the liquid nitrogen tank on the following day.

2.3. Protein determination

Sample preparation

1) Culture plate was put on ice. Culture medium was removed from the wells using micropipette.
2) The cells were washed with 2 ml ice-cold PBS.
3) Appropriate volume of ice-cold lysis buffer was added to the culture wells. The cells were scraped off using a rubber cell scraper.
4) The cell lysate was collected in eppendorf tubes and was put on ice for 30 min.
5) The cell lysate was centrifuged at 13,000 ×g for 10 min at 4°C to remove whole cells and nuclei. The post-nuclear supernatant was stored at -20°C for further use.

Protein determination

1) A standard curve (0-1.2 mg /ml of BSA) was prepared each time the assay was performed. BSA stock solution concentration was 1.2 mg/ml.
2) A total of 25 µl of standard BSA solution and the sample were added into clean, dry eppendorf tubes.
3) RC reagent I (125 µl) was added into each tube. The tubes were vortexed and incubated for 1 min at room temperature.

4) RC reagent II (125 µl) was added into each tube. The tubes were vortexed and centrifuged at 13,000 ×g for 10 min at room temperature.
5) The supernatant was discarded by inverting the tubes on clean, absorbent tissue paper. Liquid should be dried completely from the tubes.
6) DC Reagent S (5 µl) was added to each 250 µl of DC Reagent A. This solution was then referred to as Reagent A' and 127 µl Reagent A' would be required for each standard or sample assay
7) Regent A' (127 µl) was added to each tube. The tubes were vortexed and incubated at room temperature for 5 min or until precipitate is completely dissolved. The tubes should be vortexed before proceeding to the next step.
8) DC Regent B (1 ml) was added to each tube. The tubes were vortexed immediately and incubated at room temperature for 15 min.
9) The liquid was transferred into cuvettes. Absorbance was read at 750nm. The absorbance would be stable for at least 1 hour.

2.4. MTT assay

1) Human fibroblast cells were seeded on 96-well plates at the density of $1.6x10^3$ cells per well and incubated in complete DMEM medium.
2) After 24 hour, the culture media were changed and the cells were incubated in complete DMEM medium containing NB-DNJ (50µM, 100µM, 150µM) or without NB-DNJ, respectively.
3) After 72 hour's further incubation, the cells were washed with PBS for three times.

4) The cells were incubated with 0.5mg/ml MTT for 30 min. Then MTT was removed and the cells were incubated with DMSO overnight.
5) The absorbance at 570nm was measured using a 96-well multi scanner.

2.5. Lipid extraction:

1) Human fibroblast cells were seeded in 75-cm^2 flasks at the density of $2.4x10^5$ cells per flask.
2) After 48 hour, the cells were treated without or with NB-DNJ (50μM, 100μM, 150μM).
3) After further incubation for 72 hour, the cells were scraped and harvested by centrifuge at 500 x g and washed with ice-cold PBS for three times.
4) The cells were finally resuspended in 400 μl H_2O and extracted in 4ml chloroform/methanol (1:1, v/v) at 4 ^oC for 16 hour.
5) The extract was centrifuged at 15,000 x g for 15 min and 4ml supernatant was collected after centrifuge.
6) Two ml chloroform / methanol (1:1, v/v) was added to wash the pellet and the supernatant was collected after centrifugation at 15,000 x g for 15 min.
7) The two supernatants were combined and dried under N_2 stream then resuspended in 15μl chloroform/methanol (1:1, v/v).

2.6. HPTLC assay:

1) Developing solvent was prepared by mixing the chloroform /methanol /0.2%$CaCl_2$ in water (65:25:4, v/v/v) thoroughly by shaking or vortex.
2) Appropriate volume of developing solvent was added into the chamber so that it was 0.5 cm deep in the bottom of the chamber.
3) The chamber was sealed and left for 2 hour so that the atmosphere in the chamber became saturated with the developing solvent.
4) The HPTLC plate was cut into 10 cm high and pre-heated at 100°C for 1 hour before use.
5) Lipid samples in 15µl chloroform/methanol (1:1, v/v) were applied to the HPTLC plate with a Camag Nanomat 4 TLC sampler at 1 cm above the bottom. The prepared HPTLC plate was placed in the developing chamber, which was then sealed, and left undisturbed.
6) HPTLC development was stopped when the solvent was about 0.5 cm below the top of the plate.
7) The HPTLC plate was taken out of the developing chamber and air-dried.
8) To visualize the GSL bands, the plate was sprayed with orcinol-H_2SO_4 reagent and heated at 110 ^oC for 10 min immediately after spraying in the oven.
9) The plate was scanned and the densities of the bands were analyzed by AIS 3.0 software (Imaging Research Inc. St. Catharines, Ontario, Canada).

2.7. Isolation of lipid rafts

1) Human fibroblast cells were seeded in 75-cm^2 flasks at the density of $2.4x10^5$ cells per flask and incubated in complete DMEM medium.
2) After incubation for 5 days, the cells were washed three times with ice-cold PBS and lysed on ice for 30 min in 1 ml Triton X-100 (1%) lysis buffer supplemented with protease inhibitor mixture.
3) The cell lysates were homogenized with 20 strokes of the homogenizer and centrifuged for 5 min at 1000 x g at 4 °C to remove the insoluble material and nuclei.
4) The supernatant was mixed with 1 ml of 80% sucrose in lysis buffer, placed at the bottom of ultracentrifuge tubes, and overlaid with 6 ml of 30% and 3 ml of 5% sucrose in TNE lysis buffer.
5) Lysates were ultracentrifuged at 4 °C in a Beckman SW41 rotor for 16 hour at 38,000 rpm. Eleven 1-ml fractions were collected from the top.
6) Samples were analyzed to western blotting. Flotillin and caveolin were used as marker proteins of lipid rafts.

2.8. Western blotting

The resolving gel solution (10%) was mixed well and allowed to degas before ammonium persulfate and TEMED were added. All reagents were quickly mixed and poured into a mini-gel casting chamber. A depth of 2.0 cm from the top was left empty. The resolving gel was overlaid with water immediately to separate the resolving gel buffer from air and was allowed to stay for 30 min. When the resolving gel had solidified,

water was removed; the stacking gel solution (4%) was prepared and poured on top of the resolving gel. A comb was inserted into the stacking gel immediately. The stacking gel solution was allowed to stay for 30 min to solidify. After the stacking gel solidified, the comb was removed.

Samples of equal volume (35µl) of individual fractions or 5µl of precision protein standard were loaded into each well of the gel. The gel was then electrophoresised at 40 volt when the dye advanced in the stacking gel. The voltage was adjusted to 100 volt when the dye entered the resolving gel. The electrophoresis was terminated till the dye front ran near the bottom of the resolving gel. The resolving gel was removed from gel casting chamber and soaked in the pre-cooled transfer buffer together with the PVDF membrane, sponge and filter paper of the same size as the gel for about 10 min. The gel sandwich was stacked in the order of sponge, filter paper, gel, membrane, filter paper and sponge. The proteins were transferred from gel onto PVDF membrane at 100 volt for 90 min at 4 °C. The membrane was then blocked in blocking buffer overnight at 4 °C and then incubated in 10ml of blocking buffer containing 1:1000 diluted anti - caveolin-1 antibody or 1:1000 diluted anti – flotillin-1 antibody for 1 hour at room temperature with shaking. The membrane was then washed with TBST buffer for four times to remove the excess first antibody and then incubated for 1 hour in TBS buffer containing 1:2500 diluted goat anti-rabbit antibody for detection of caveolin-1 or 1:3000 diluted goat anti-mouse antibody for detection of flotillin-1. The membrane was then thoroughly washed with TBST buffer for four times to remove the excess secondary antibody. Finally the membrane was submerged in a mixture of equal volume of super signal west pico

chemiluminescent substrate and enhancer for 1 min before it was removed from the mixture and placed against the film in the cassette. The film was developed after appropriate exposure by following the manufacturer's instructions.

2.9. $DiIC_{18}$ staining

Preparation of labeling reagent

1) $DiIC_{18}$ (1 mg) was diluted in 400ul ethanol then injected, while vortexing, into an equimolar amount of fatty acid-depleted BSA in 1 ml PBS at pH 7.4. This mixture was then dialyzed thoroughly against several changes of PBS.
2) The dialysate was centrifuged at 100,000 x g for 20 min and the supernatant was collected. This supernatant was centrifuged at 100,000 x g for 20 min again and the pellet was disposed.
3) The $DiIC_{18}$-loaded BSA solutions were sterilized by passage through 0.2-μm syringe filters and stored at 4°C.
4) The labeling reagent was centrifuged at 100,000 x g for 20 min immediately before use every time.

$DiIC_{18}$ labeling

1) Human fibroblast cells were seeded on coverslips in 24-well plates at the density of $4x10^3$ cells per well and incubated in complete DMEM medium.
2) After 24 hour, the culture medium was replaced by complete DMEM medium with 50μM NB-DNJ or without NB-DNJ, respectively.

3) After further incubation for 72 hour, the cells were washed with medium 1 at 37 ^{o}C for three times and labeled with 10μM $DiIC_{18}$ at 37 ^{o}C for 20 sec.
4) The cells were then quickly washed with ice-cold medium 1 for three times and extracted with 1% Triton X 100 on ice for 20 min. For the control group, the cells were incubated with medium 1 on ice for 20 min.
5) After extraction, the cells were washed with cold medium 1 twice and slightly fixed with 2% PFA on ice for 10 min.
6) After the fixation, the cells were washed with cold PBS for three times and the coverslips were mounted on slides.

Confocal microscope

Confocal microscopy was performed using an Olympus FLVOVIEW 500 inverted microscope. Cells labeled with $DiIC_{18}$ were excited with a HeNe laser emitting at 543nm and a 560nm long pass filter was used for collecting emissions. Images were acquired using a x40 oil objective. For quantitative analysis, images were processed with the Image–Pro Plus software (EPIX Inc. Buffalo Grove, IL, USA). Images were quantified by manually outlining each cell and taking the average fluorescence intensity associated with the cells. The ratio of average fluorescence intensity obtained from the extracted cells and the control was determined as the percentage of ordered raft domains.

2.10. CTxB binding

1) Human fibroblast cells were seeded on coverslips in 24-well plates at the density of $4x10^3$ cells per well and incubated in complete DMEM medium.
2) After further incubation for 72 hour, the cells were washed with ice-cold PBS for 3 times and labeled with 7.5μg/ml CTxB conjugated with Alexa Fluor 594 at 0 ^oC for 10 min.
3) For one group, the cells were quickly washed with cold PBS for three times and fixed with 2% PFA on ice for 10 min.
4) For another group, the cells were washed with cold PBS for three times and incubated at 37 ^oC for 5 min to initiate the uptake of CTxB by the cells. Then the cells were fixed with 2% PFA on ice for 10 min.
5) After fixation, the cells were washed with ice-cold PBS for three times and the coverslips were mounted on slides.
6) Fluorescent CTxB was observed under Olympus IX71 fluorescence microscope using a 560nm (55nm bandpass) excitation filter and a 645nm (75nm bandpass) emission filter. Images were acquired using a x40 objective.

2.11. Flow cytometry

CTxB labeling

1) Human fibroblast cells were seeded in 25-cm^2 flasks at the density of $8x10^4$ cells per flask and incubated in complete DMEM medium.
2) After 24 hour, the cells were incubated in complete DMEM medium with NB-DNJ (50μM, 100μM, 150μM) or without NB-DNJ, respectively.

3) After further incubation for 72 hour, the cells were scraped and harvested by centrifuge at 500 x g. Then the cells were washed with buffer A for three times.
4) Then cells were resunspended in 50ul buffer A. Then the cells were labeled with 5μg of CTxB conjugated with Alexa Fluor 488 in dark at 0 ^{o}C for 30 min.
5) The cells were washed twice with buffer A and resuspended in 1ml buffer A containing propidium iodide (2μg/ml). Then the samples were analyzed by flow cytometry.

Flow cytometry

Samples were analyzed on a Beckman Coulter flow cytometer (Epics Altra) using a 488nm excitation laser. A 530nm (40nm bandpass) filter was used to collect the emission of CTxB conjugated with Alexa Fluor 488 and a 613nm (20nm bandpass) filter was used to collect the emission of PI. Data were collected on 10^4 viable cells and plotted on a four-decade $\log_{10}$ scale of increasing fluorescence intensity on the x-axis. Dead cells and cellular debris were excluded from the analysis on the basis of different uptake of PI and a size gate. The relative fluorescence intensity percentage was obtained by dividing the geometric mean fluorescence intensity of the treated cells by that of the control cells.

2.12. CTxB endocytosis

1) Human fibroblast cells were seeded on coverslips in 24-well plates at the density of $4x10^3$ cells per well and incubated in complete DMEM medium.

2) After 24 hour, the cells were incubated in complete DMEM medium with NB-DNJ (50μM, 100μM, 150μM) or without NB-DNJ, respectively.
3) After further incubation for 72 hour, the cells were washed with warm PBS for three times. Then the cells were labeled with CTxB (7.5μg/ml) conjugated with Alexa Fluor 594 at 37 ^{o}C for 5 min, 10 min or 15 min, respectively.
4) Then the cells were quickly washed with cold PBS for three times and fixed with 2% PFA on ice for 10 min followed by 20min fixation with 2% PFA at room temperature.
5) After fixation, the cells were washed for three times with PBS and the coverslips were mounted on slides.
6) Fluorescent CTxB was observed under Olympus IX71 fluorescence microscope using a 560nm (55nm bandpass) excitation filter and a 645nm (75nm bandpass) emission filter. Images were acquired using a x10 objective.
7) For quantitative analysis, images were processed with the Image–Pro Plus software (EPIX Inc. Buffalo Grove, IL, USA). Images were quantified by manually outlining each cell and taking the average fluorescence intensity associated with the cells.
8) The relative percentage of fluorescence intensity was obtained by dividing average fluorescence intensity of the treated cells by that of the control cells.

2.13. Filipin staining

2.13.1. Effect of progesterone on intracellular trafficking of cholesterol

1) Human fibroblast cells were seeded on coverslips in 24-well plates at the density of $4x10^3$ cells per well and incubated in complete DMEM medium.
2) After 72 hour, the medium was replaced and the cells were incubated in the presence or absence of LDL (50μg/ml) and progesterone (5μg/ml, 10μg/ml or 20μg/ml), respectively.
3) After 24 hour, the cells were washed with warm PBS for three times and fixed in 4% PFA at 37 ^oC for 25 min.
4) Then the cells were washed with warm PBS for three times and stained with filipin (50μg/ml) at 37 ^oC for 30 min.
5) Then the cells were washed with PBS for three times and the coverslips were mounted on slides.
6) Filipin fluorescence was observed under Olympus IX71 fluorescence microscope using a 330-385nm excitation filter and a 420nm emission filter. Images were acquired using a x20 objective.

2.13.2, Effect of NB-DNJ on intracellular trafficking of cholesterol in normal cells

1) Human fibroblast cells were seeded on coverslips in 24-well plates at the density of $4x10^3$ cells per well and incubated in complete DMEM medium.
2) After 48 hour, the medium was replaced and the cells were incubated in the presence or absence of LDL (50μg/ml) and NB-DNJ (50μM, 100μM, 150μM), respectively.

3) After 72 hour, the cells were washed with warm PBS for three times and fixed in 4% PFA at 37 ^{o}C for 25 min.
4) Then the cells were washed with warm PBS for three times and stained with filipin (50μg/ml) at 37 ^{o}C for 30 min.
5) Then the cells were washed with PBS for three times and the coverslips were mounted on slides.
6) Filipin fluorescence was observed under Olympus IX71 fluorescence microscope using a 330-385nm excitation filter and a 420nm emission filter. Images were acquired using a x20 objective.

2.13.3. Effect of NB-DNJ on intracellular trafficking of cholesterol in NPC-like cells

1) Human fibroblast cells were seeded on coverslips in 24-well plates at the density of $4x10^3$ cells per well and incubated in complete DMEM medium.
2) After 48 hour, the medium was replaced and the cells were incubated in the presence or absence of LDL (50μg/ml) and NB-DNJ (50μM, 100μM, 150μM), respectively.
3) After 48 hour, the medium was replaced by medium with NB-DNJ (50μM, 100μM, 150μM) or without NB-DNJ, supplementary with 50μg/ml LDL and 10μg/ml progesterone.
4) After 24 hour, the cells were washed with warm PBS for three times and fixed in 4% PFA at 37 ^{o}C for 25 min.

5) Then the cells were washed with warm PBS for three times and stained with filipin (50μg/ml) at 37 ^{o}C for 30 min.
6) Then the cells were washed with PBS for three times and the coverslips were mounted on slides.
7) Filipin fluorescence was observed under Olympus IX71 fluorescence microscope using a 330-385nm excitation filter and a 420nm emission filter. Images were acquired using a x20 objective.

CHAPTER 3. RESULTS

3.1. Effect of NB-DNJ on GSL biosynthesis in human fibroblast cells

3.1.1. Cellular toxicity of NB-DNJ in human fibroblast cells

MTT [3-(4,5-dimethylthiazol-2-yl)-2,5-diphenyltetrazolium bromide] assay is based on the ability of a mitochondrial dehydrogenase enzyme from viable cells to cleave the tetrazolium rings of the pale yellow MTT and form a dark blue formazan crystals which is largely impermeable to cell membranes, resulting in its accumulation within healthy cells. The number of surviving cells is directly proportional to the level of the formazan produced. The color can then be quantified using a simple colorimetric assay (Mosmann, 1983). In this study, MTT assay was employed to assess the toxicity of NB-DNJ in human fibroblast cells. Table 3.1 shows that NB-DNJ, even at the highest concentration of 150μM used here, had no detectable toxicity on human fibroblast cells. The results suggest that NB-DNJ provides a safe approach to manipulate GSL level in the cells.

Sample	Absorbance
Control cells	0.6071 ± 0.0167
50 μM NB-DNJ treated cells	0.5888 ± 0.0114
100μM NB-DNJ treated cells	0.5945 ± 0.0094
150μM NB-DNJ treated cells	0.6012 ± 0.0096

Table.3.1 Cellular toxicity of NB-DNJ in human fibroblast cells. Human fibroblast cells were incubated in complete DMEM medium with NB-DNJ (50μM, 100μM, 150μM) or

without NB-DNJ, respectively. The cells were then treated with 0.5mg/ml MTT for 30 min. MTT was removed and the cells were incubated with DMSO overnight. The absorbance at 570nm was measured. Data was presented as mean ± S.D.

3.1.2. Effect of NB-DNJ on ganglioside biosynthesis in human fibroblast cells.

The Imino sugar NB-DNJ is an inhibitor of the Cer-specific glucosyltransferase that catalyzes the first step in GSL biosynthesis, resulting in extensive GSL depletion in vitro (Platt, et al, 1993). The effect of NB-DNJ on GSL biosynthesis in human fibroblast cells was studied by incubating the cells in the presence of different doses of NB-DNJ (50 μM, 100μM, 150μM) or in the absence of NB-DNJ. The cellular GSL content was examined by HPTLC. Figure 3.1 and Figure 3.2 show that GM3 is the major GSL species in the human fibroblast cells. The amount of GM3 in the human fibroblast cells was significantly reduced by 70% in the presence of 50μM NB-DNJ. This inhibition activity of NB-DNJ was dose dependent. When the dose of NB-DNJ was increased to 150μM, the amount of GM3 in the human fibroblast cells was decreased by up to 80%. These results suggest that NB-DNJ had efficiently depleted GSL, at least GM3, in the human fibroblast cells. Due to the limitation of the sensitivity of HPTLC, the change of other species of GSLs could not be detected by HPTLC.

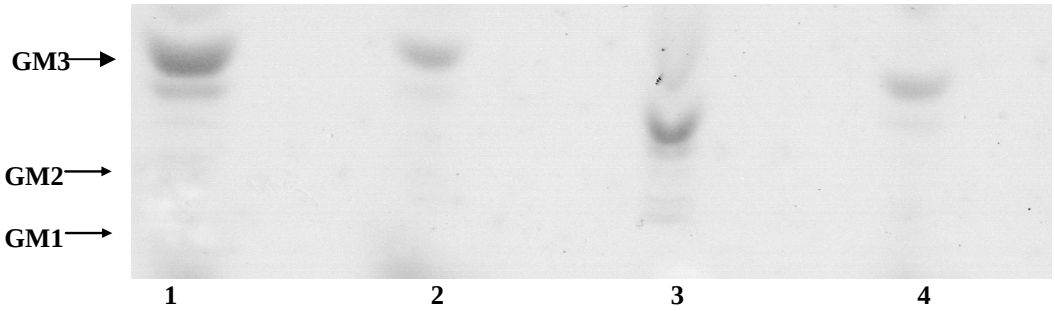

Fig. 3.1 Effect of NB-DNJ on ganglioside biosynthesis in human fibroblast cells. Human fibroblast cells were incubated in complete DMEM medium with NB-DNJ (50μM, 100μM, 150μM) or without NB-DNJ respectively. Total lipids extraction and HPTLC assay were conducted according to the procedure described in Materials and Methods. GSL bands were visualized by spraying with Orcinol-H_2SO_4 reagent and heated at 110 ^oC for 10 min. GM1, GM2 and GM3 standards (1μg) were used as the markers. Lane 1: Control cells; Lane 2: 50μM NB-DNJ treated cells; Lane 3: 100μM NB-DNJ treated cells; Lane 4: 150μM NB-DNJ treated cells.

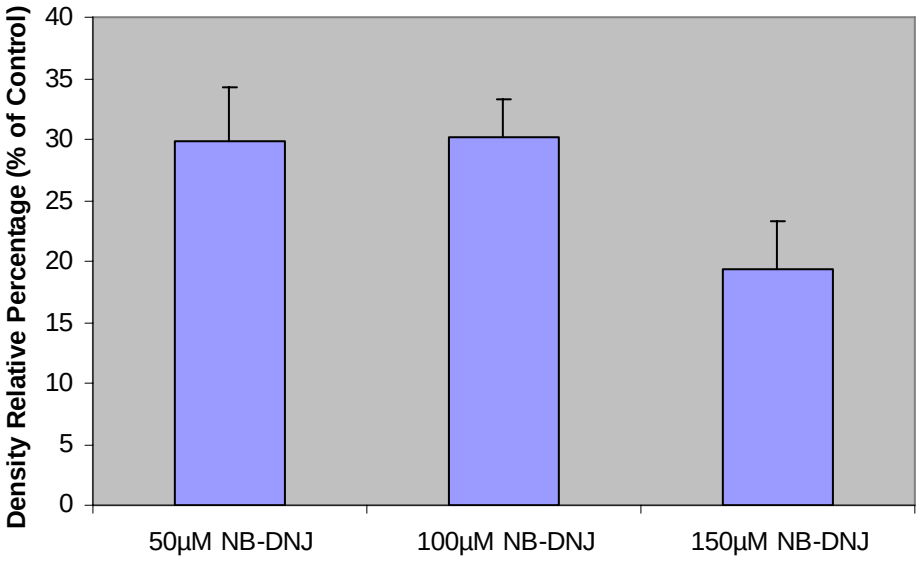

Fig. 3.2 Effect of NB-DNJ on GM3 biosynthesis in human fibroblast cells. Human fibroblast cells were incubated in complete DMEM medium with NB-DNJ (50μM, 100μM, 150μM) or without NB-DNJ, respectively. Total lipid extraction and HPTLC assay were conducted according to the procedure in Materials and Methods. GSL bands were visualized by spraying with Orcinol-H_2SO_4 reagent and heated at 110 ^oC for 10 min. The densities of the GM3 bands for the control cells and the NB-DNJ treated cells were quantified. The relative percentage of density was obtained by dividing the density of the GM3 band for the NB-DNJ treated cells by that of the control cells. The density of the GM3 band for the control cells was set as 100%. Data was presented as mean ± S.D.

3.1.3. Effect of NB-DNJ on cell surface GM1 in human fibroblast cells.

Cholera toxin belongs to a family of structurally homologous hexameric AB_5 bacterial toxins (Lindberg, et al., 1987). The B subunit of cholera toxin (CTxB) specifically binds the ganglioside GM1 at the cell surface and may associate with the lipid rafts (Spangler, 2002). The CTxB binding thus could reflect the level of GM1 at the cell surface. In this study, human fibroblast cells were treated with NB-DNJ (50μM, 100μM, 150μM) or without NB-NBJ. Then the cells were labeled with CTxB (7.5μg/ml) conjugated with Alexa Fluor 594. And the effect of NB-DNJ on the GM1 at the cell surface was evaluated by examining the CTxB bound to the cells by using flow cytometry. Figure 3.3 shows that fluorescent CTxB was localized at the plasma membrane and little CTxB were internalized into the cells at 0 ^{o}C while CTxB were observed to distribute in the intracellular organelles at 37 ^{o}C. This result suggests that CTxB bound to the GM1 at the plasma membrane at 0 ^{o}C and were internalized at 37 ^{o}C. Thus the CTxB binding at 0 ^{o}C might be used to reflect the GM1 level at the cell surface. Figure 3.4 and Figure 3.5 show that the level of CTxB bound to the cells was reduced by 45% in the presence of 50μM NB-DNJ. When the dose of NB-DNJ was increased to 150μM, the level of CTxB bound to the cells was decreased by up to 65%. These results suggest that in the presence of NB-DNJ, the GM1 at the cell surface was significantly decreased, which provides further evidence for the inhibitory effect of NB-DNJ on GSL biosynthesis in human fibroblast cells.

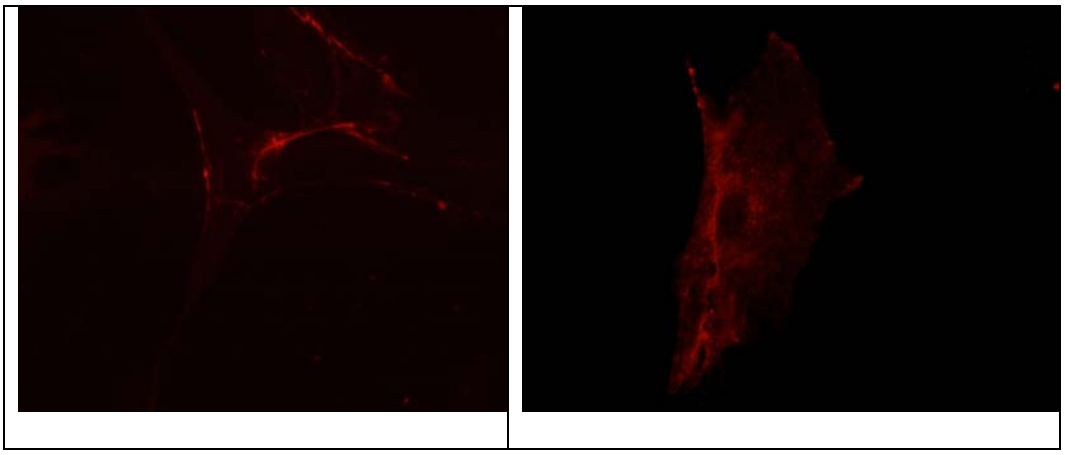

A **B**

Fig. 3.3 The different behaviors of CTxB at 0 ^{o}C and 37 ^{o}C in human fibroblast cells. **A**, Human fibroblast cells were incubated in complete DMEM medium. Cells were labeled with 7.5µg/ml CTxB conjugated with Alexa Fluor 594 at 0 ^{o}C for 10 min. Then the cells were washed and fixed with 2% PFA on ice for 10 min; **B** Human fibroblast cells were incubated in complete DMEM medium. Cells were labeled with 7.5µg/ml CTxB conjugated with Alexa Fluor 594 at 0 ^{o}C for 10 min. Then the cells were incubated at 37 ^{o}C for 5 min to initiate the uptake of CTxB by the cells. Then the cells were fixed with 2% PFA on ice for 10 min. Fluorescent CTxB was observed under fluorescence microscope according to the procedure described in Materials and Methods.

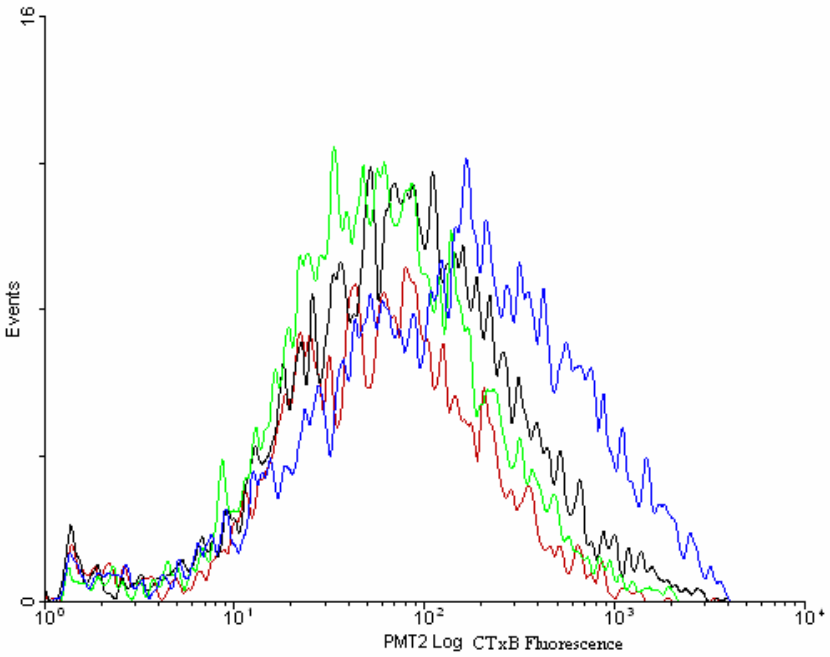

---- Control cells
---- 50µM NB-DNJ treated cells
---- 100µM NB-NDJ treated cells
---- 150µM NB-DNJ treated cells

Fig 3.4 Effect of NB-DNJ on cell surface GM1 in human fibroblast cells. Human fibroblast cells were incubated in complete DMEM medium with NB-DNJ (50µM, 100µM, 150µM) or without NB-DNJ respectively. Cells were labeled with 5µg CTxB conjugated with Alexa Fluor 488 in dark at 0 ^{o}C for 30 min. Cells were resuspended in 1 ml buffer A containing 2µg/ml PI for flow cytometry analysis. Data were collected on 10^4 viable cells and plotted on a four-decade $\log_{10}$ scale of increasing fluorescence intensity on the x-axis. Dead cells and cellular debris were excluded from the analysis on the basis of different uptake of PI and a size gate.

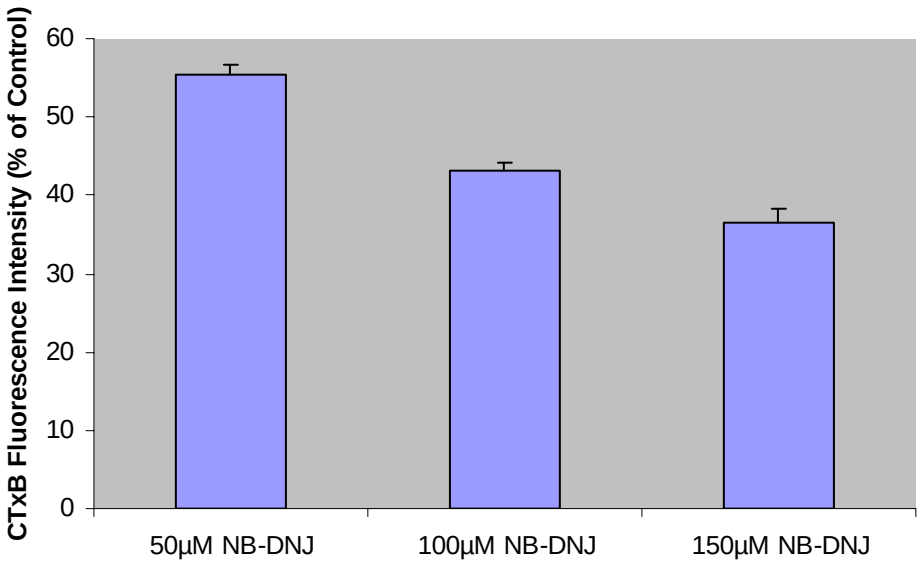

Fig. 3.5 Effect of NB-DNJ on cell surface GM1 in human fibroblast cells. CTxB staining and flow cytometry analysis were conducted according to the procedure described in Materials and Methods. The relative percentage of fluorescence intensity was obtained by dividing the geometric mean fluorescence intensity of the NB-DNJ treated cells by that of the control cells. The fluorescence intensity of control cells was set as 100%. Data was presented as mean ± S.D.

3.2. Effect of NB-DNJ on raft formation in human fibroblast cells

3.2.1. Isolation of lipid rafts from human fibroblast cells

Lipid rafts could be extracted as DRMs from the cell lysis on the basis of their insolubility in Triton X-100 at 4°C and their ability to float in sucrose density gradients (Hering, et al., 2003). Lipid raft-containing fractions were tracked by the cholesterol binding protein caveolin-1 and the raft integral membrane protein flotillin-1, which are generally regarded as markers of lipid rafts (Hering, et al., 2003). Figure 3.6 shows that flotillin-1 and caveolin-1 both peaked at light fractions (f3-f4). Caveolin-1 had an additional peak at heavier fractions (f10-f11). These results shows that lipid rafts exist in human fibroblast cells and rafts were enriched in the light fractions of the sucrose gradient.

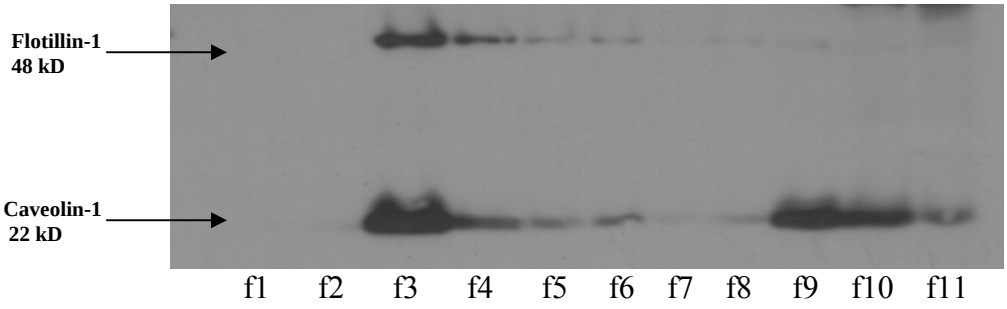

Fig. 3.6 Isolation of lipid rafts from human fibroblast cells. Human fibroblast cells were incubated in complete DMEM medium. The cell lysate was extracted by cold Triton X-100 according to the procedure described in Materials and Methods. Extract was applied to sucrose gradient and centrifuged in a Beckman SW41 rotor at 38,000 rpm for 16 hour at 4 °C. Eleven 1-ml fractions were collected from the top (f1) of the gradient. The distribution of flotillin-1 and caveolin-1 were examined by Western blot according to the procedure described in Materials and Methods. f1-f11: fraction1 –fraction 11.

3.2.2. Effect of NB-DNJ on raft formation in human fibroblast cells

It is suggested that raft domains are resistant to cold Triton X-100 extraction while non-raft domains are soluble. In living cells, lipid analog $DiIC_{18}$ has been shown to preferentially partition into liquid ordered domains of membrane and remain associated with the cells after Triton X-100 extraction (Sun, et al., 2003). In this study, to investigate the effect of NB-DNJ on raft formation, human fibroblast cells were incubated with NB-DNJ (50μM) or without NB-DNJ respectively. Then the cells were labeled with $DiIC_{18}$ (10μM) and extracted with cold Triton X-100. The ratio of average fluorescence intensity of $DiIC_{18}$ obtained from Triton X-100 extracted cells to that of the control cells was assumed to represent the percentage of raft domains. Figure 3.7 shows that $DiIC_{18}$ efficiently partitioned into the plasma membrane in both control cells and NB-DNJ treated cells. After Triton X-100 extraction the fluorescent $DiIC_{18}$ associated with the cells were decreased more significantly in the NB-DNJ treated cells than that in the control cells. Figure 3.8 shows that, after GSL depletion by NB-DNJ treatment, the raft domains percentage was decreased by 20% in human fibroblast cells, suggesting that GSL was essential for raft formation in human fibroblast cells.

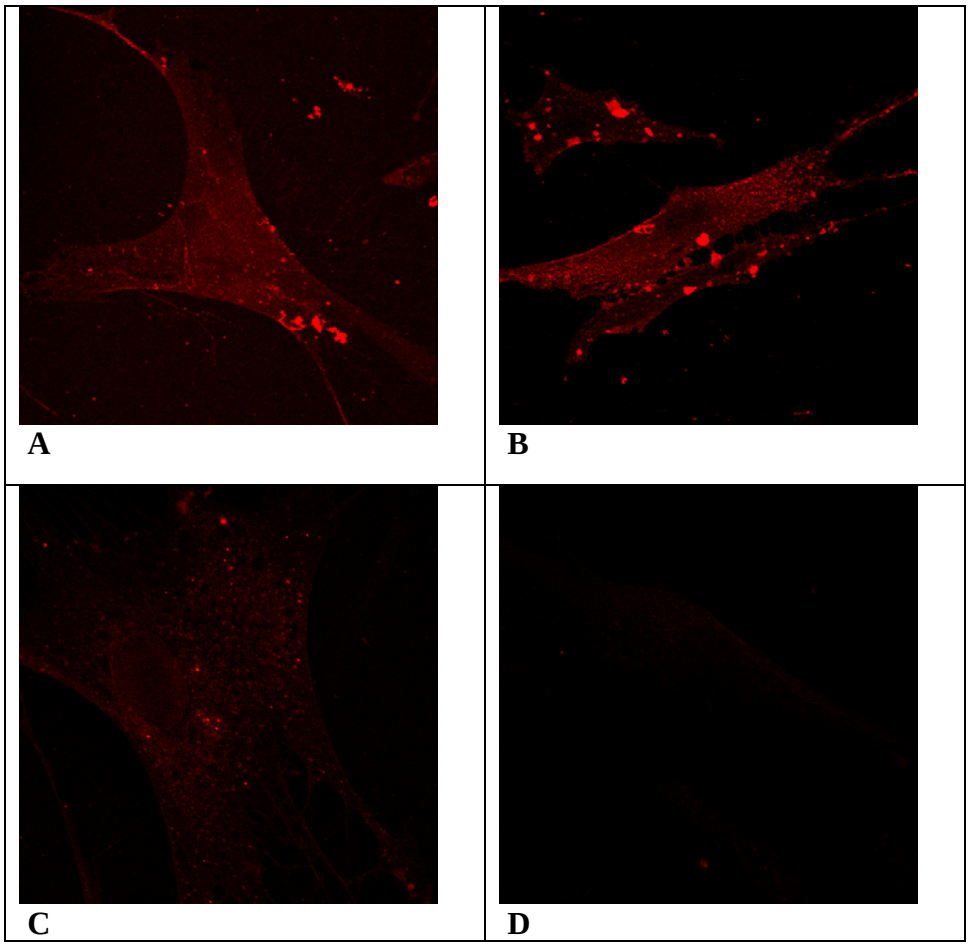

A: Control cells without Triton X-100 extraction

B: 50µM NB-DNJ treated cells without Triton X-100 extraction

C: Control cells extracted with Triton X-100 extraction

D: 50µM NB-DNJ treated cells extracted with Triton X-100

Fig. 3.7 Human fibroblast cells labeled with $DiIC_{18}$. Human fibroblast cells were incubated in complete DMEM medium with 50µM NB-DNJ or without NB-DNJ respectively. The cells were labeled with 10µM $DiIC_{18}$ at 37 ^{o}C for 20 sec. In **A** and **B**: The cells were incubated with medium 1 without Triton X-100 on ice for 20 min. in **C** and **D:** The cells were extracted with 1% Triton X-100 in medium 1 on ice for 20 min. The samples were subsequently fixed and mounted on coverslips. Fluorescent $DiIC_{18}$ was examined by confocal microscope according to the procedure described in Materials and Methods.

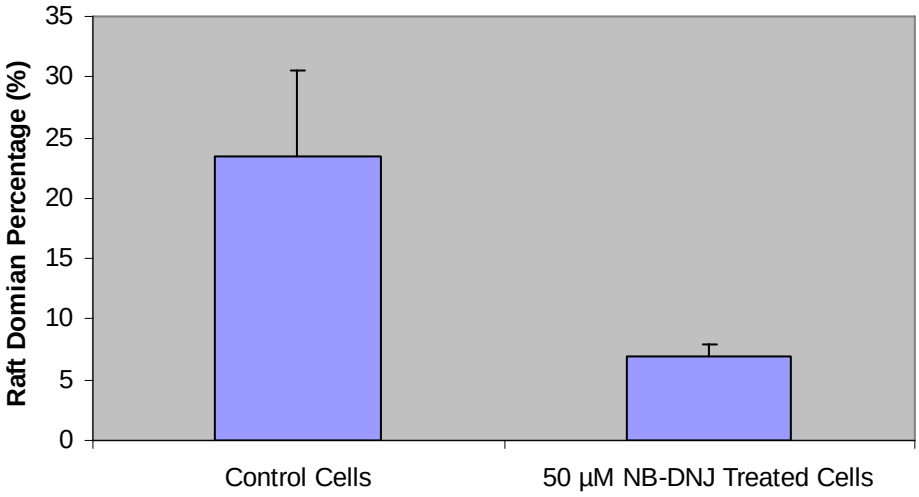

Fig. 3.8 Effect of NB-DNJ on raft formation in human fibroblast cells. The data were generated from the ratios of the average $DiIC_{18}$ fluorescence intensities obtained from the Triton X-100 extracted cells to the average $DiIC_{18}$ fluorescence intensities of the cells without Triton X-100 extraction (similar to that shown in Fig 3.7). Images were quantified by manually outlining each cell and taking the average fluorescence intensity associated with the cells. Eighteen cells were counted under each condition. *P = 0.016* Data was presented as mean ± S.D.

3.3. Effect of NB-DNJ on CTxB endocytosis in human fibroblast cells

CTxB is suggested to be internalized via the caveolae/raft dependent endocytosis pathway (Pelkmans and Helenius, 2002). In this study, human fibroblast cells were treated with different doses of NB-DNJ (50μM, 100μM, 150μM) and the endocytosis of fluorescence conjugated CTxB was examined to evaluate the effect of NB-DNJ treatment on raft function. Figure 3.10 to Figure 3.12 show that fluorescent CTxB associated with the cells increased following incubation of the cells with CTxB for 5 – 15 min, suggesting that CTxB was continuously taken up by the cells. Furthermore, CTxB endocytosis was significantly inhibited by NB-DNJ in a dose-dependent manner after incubation of 5-15 min. Figure 3.13 shows that in the presence of 50μM NB-DNJ, the CTxB internalized by the cells was decreased by up to 40%. When the dose of NB-DNJ was increased to 150μM, the CTxB endocytosis was decreased by up to 65%. The results suggest that formation of lipid rafts was inhibited by the GSL biosynthesis inhibitor, NB-DNJ, which in turn inhibited the CTxB endocytosis via the caveolae/raft endocytosis pathway.

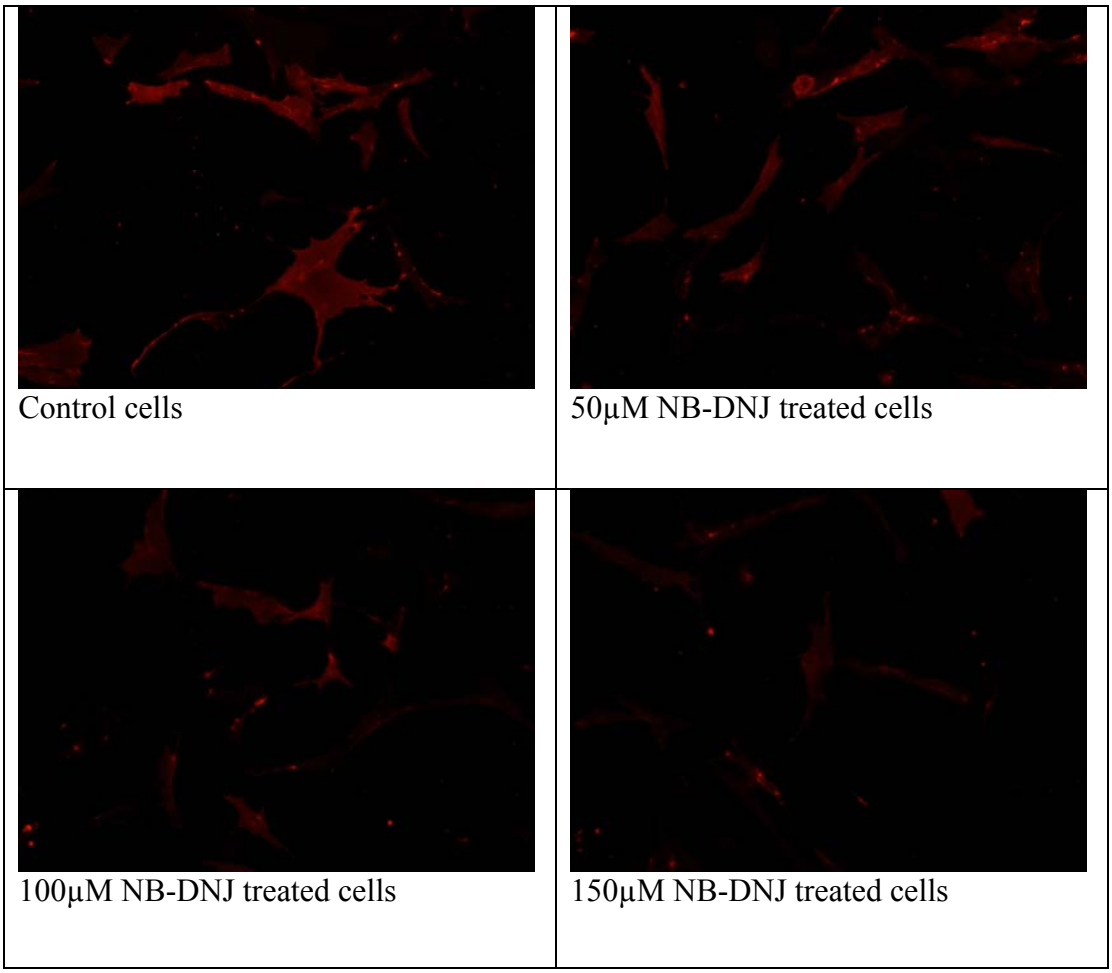

Fig. 3.9 Effect of NB-DNJ on CTxB endocytosis in human fibroblast cells**.** Human fibroblast cells were incubated in complete DMEM medium with NB-DNJ (50μM, 100μM, 150μM) or without NB-DNJ respectively. Cells were labeled with 7.5μg/ml CTxB conjugated with Alexa Fluor 594 at 37 ^{o}C for 5 min. Fluorescent CTxB was observed according to the procedure in Materials and Methods.

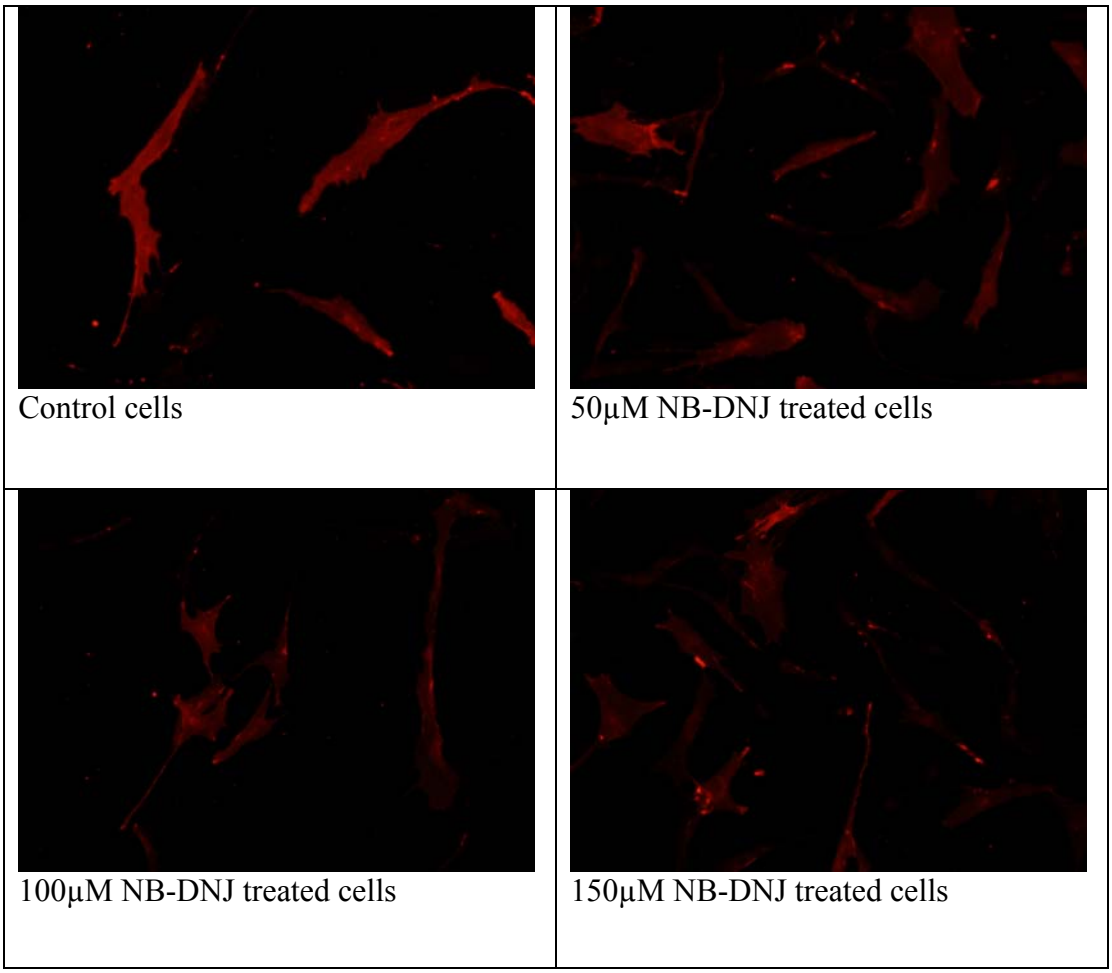

Fig. 3.10 Effect of NB-DNJ on CTxB endocytosis in human fibroblast cells**.** Human fibroblast cells were incubated in complete DMEM medium with NB-DNJ (50μM, 100μM, 150μM) or without NB-DNJ respectively. Cells were labeled with 7.5μg/ml CTxB conjugated with Alexa Fluor 594 at 37 ^{o}C for 10 min. Fluorescent CTxB was observed according to the procedure described in Materials and Methods.

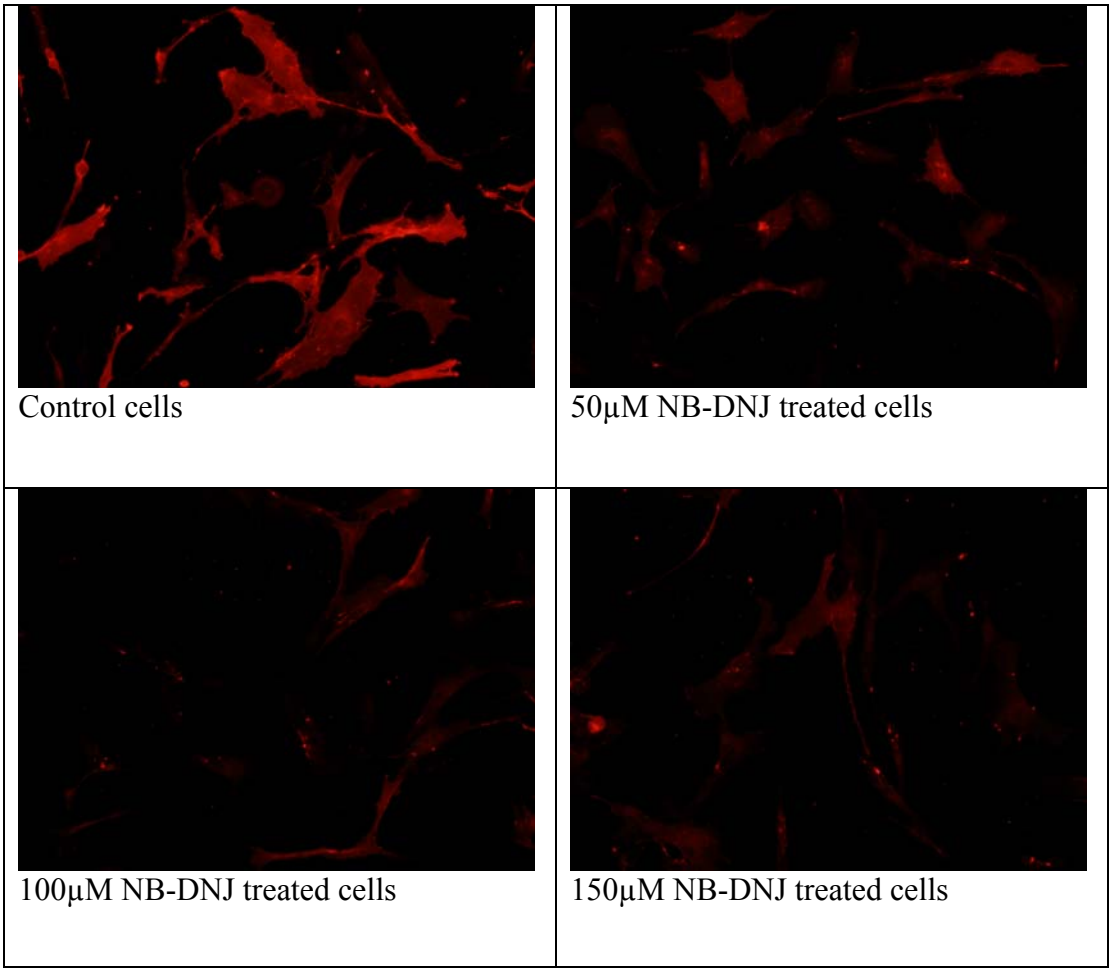

Fig. 3.11 Effect of NB-DNJ on CTxB endocytosis in human fibroblast cells**.** Human fibroblast cells were incubated in complete DMEM medium with NB-DNJ (50μM, 100μM, 150μM) or without NB-DNJ respectively. Cells were labeled with 7.5μg/ml CTxB conjugated with Alexa Fluor 594 at 37 ^{o}C for 15 min. Fluorescent CTxB was observed according to the procedure in Materials and Methods.

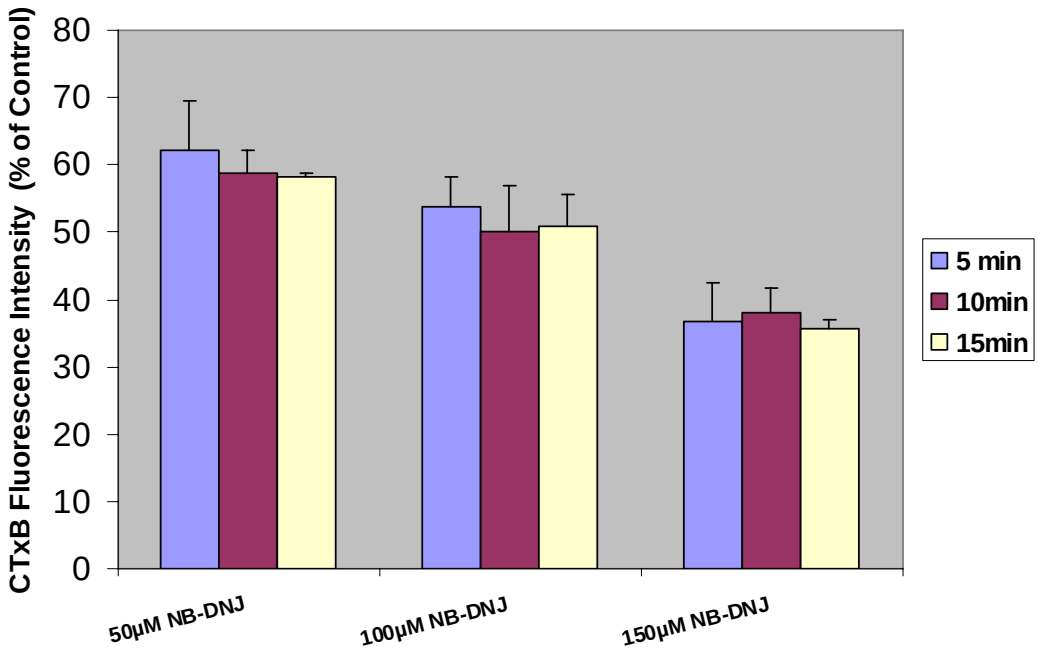

Fig. 3.12 Effect of NB-DNJ on CTxB endocytosis in human fibroblast cells**.** Human fibroblast cells were incubated in complete DMEM medium with NB-DNJ (50μM, 100μM, 150μM). CTxB staining and fluorescence microscope examination were conducted according to the procedure described in Materials and Methods. Images were quantified by manually outlining each cell and taking the average fluorescence intensity associated with the cells. Twenty cells were counted under each condition. The relative percentage of the fluorescence intensity was obtained by dividing the average fluorescence intensity of the NB-DNJ treated cells by that of the control cells. The fluorescence intensity of the control cells was set as 100%. Data was presented as mean ± S.D.

3.4. Effect of NB-DNJ on intracellular cholesterol trafficking in human fibroblast cells

3.4.1. Effect of progesterone on intracellular trafficking of cholesterol in human fibroblast cells

Progesterone has been reported to induce intensive cholesterol accumulation in the LE and LY in normal cells and cytochemically the intracellular accumulation of cholesterol in progesterone-treated cells is indistinguishable from the cholesterol accumulation in the LE and LY in NPC cells (Blanchette-Mackie, et al., 1988). As a control experiment, human fibroblast cells were treated with progesterone, following excessive loading of LDL. The intracellular distribution of cholesterol was examined by filipin staining. Figure 3.14 shows that in the presence of 10μg/ml progesterone, intense filipin-cholesterol staining was observed in perinuclear vacuoles which are the LE and LY. Our results reveal that progesterone efficiently induced cholesterol accumulation in the LE and LY and the intracellular accumulation of cholesterol in progesterone-treated cells was indistinguishable from the cholesterol accumulation in LE and LY in NPC cells. 10μg/ml progesterone was used to induce cholesterol accumulation in the following experiments.

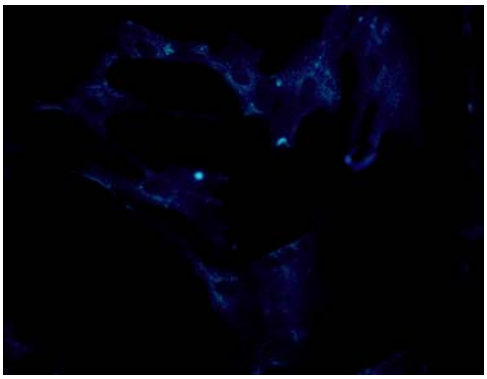

Control cells

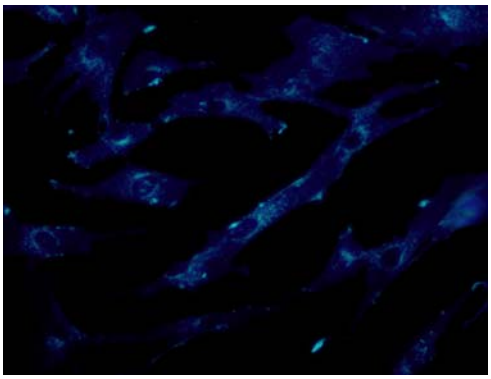

50µg/ml LDL

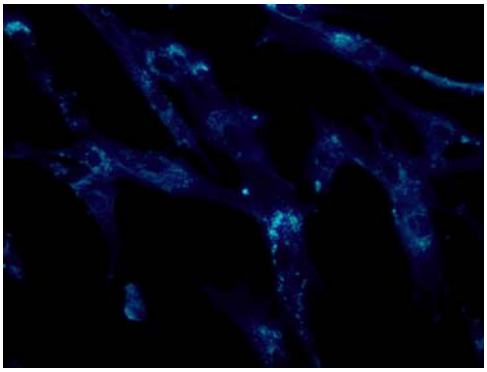

50µg/ml LDL+ 5µg/ml Progesterone

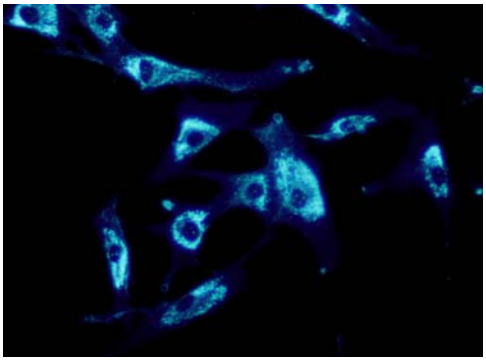

50µg LDL +10µg/ml Progesterone

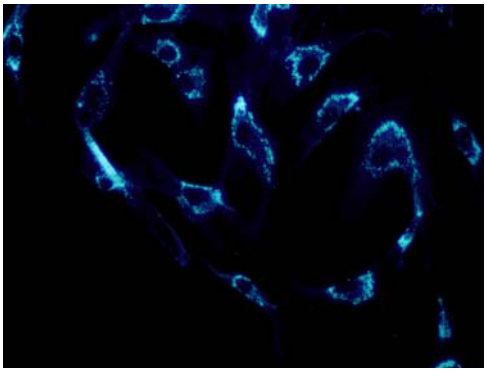

50µg/ml LDL + 20µg/ml Progesterone

Fig. 3.13 Effect of progesterone on intracellular trafficking of cholesterol in human fibroblast cells. Human fibroblast cells were incubated in the presence or absence of LDL (50µg/ml) and progesterone (5µg/ml, 10µg/ml, 20µg/ml) respectively. The cells were labeled with 50µg/ml filipin at 37 ^{o}C for 30 min. Filipin staining was observed under fluorescence microscope according to the procedure described in Materials and Methods.

3.4.2. Effect of NB-DNJ on intracellular trafficking of cholesterol in human fibroblast cells

It has been reported that the cholesterol accumulation in NPC cells might be ganglioside dependent (Marjorie, et al, 2003). It was suggested that lipid rafts in the endocytic pathway might play a role in the regulation of cholesterol trafficking (Simons and Gruenberg, 2000). To verify this hypothesis, the effect of NB-DNJ on intracellular cholesterol trafficking was investigated in both normal cells and NPC-like cells. Our previous data (Figure 3.14) shows that progesterone induced intensive cholesterol accumulation in the LE and LY of the normal human fibroblast cells, which is cytochemically indistinguishable from the cholesterol accumulation in the LE and LY of the NPC cells. Thus progesterone treated cells were employed as NPC-like cells in this study. Figure 3.15 shows that in the normal cells, both in the presence and absence of NB-DNJ, the pattern of the distribution of intracellular cholesterol were similar. Figure 3.16 shows that both in the presence and absence of NB-DNJ, progesterone induced intensive cholesterol accumulation in the LE and LY and NB-DNJ did not significantly relieve the cholesterol accumulation in the LE and LY of the NPC-like cells. Our results suggest that the decrease of GSLs alone did not affect the intracellular trafficking of cholesterol and rafts might not directly mediate the intracellular cholesterol trafficking.

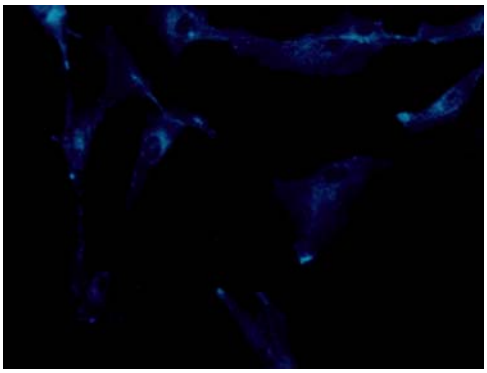

Control cells

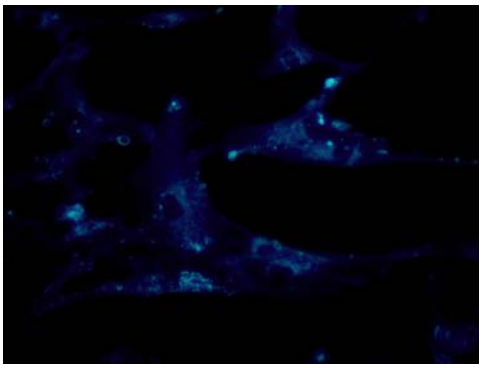

50µg/ml LDL

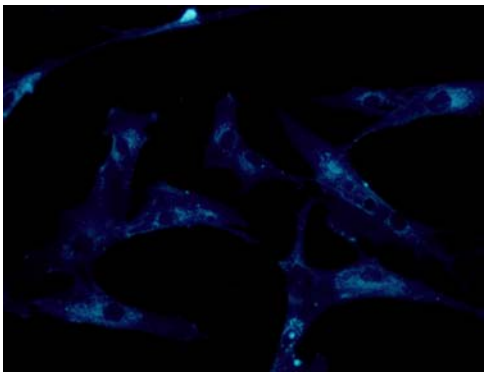

50µg/ml LDL + 50µM NB-DNJ

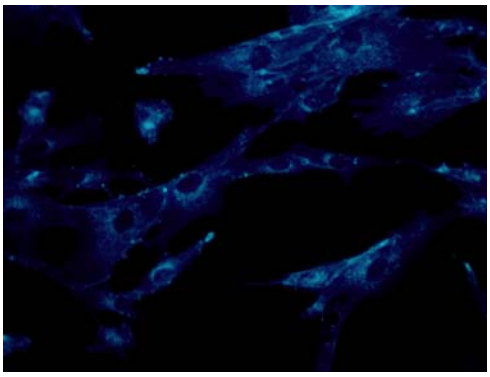

50µg/ml LDL + 100µM NB-DNJ

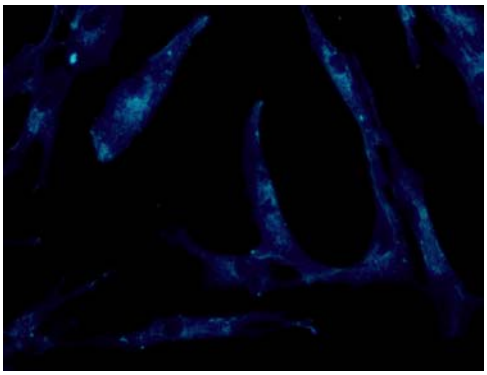

50µg/ml LDL + 150µM NB-DNJ

Fig. 3.14 Effect of NB-DNJ on intracellular trafficking of cholesterol in normal human fibroblast cells. Human fibroblast cells were incubated with NB-DNJ (50µM, 100µM, 150µM) or without NB-DNJ respectively. After incubation for 72 hour the cells were labeled with 50µg/ml filipin at 37 ^{o}C for 30 min. Filipin staining was observed under fluorescence microscope according to the procedure described in Materials and Methods.

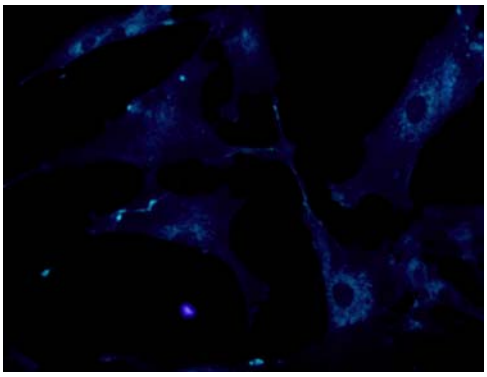

Control cells

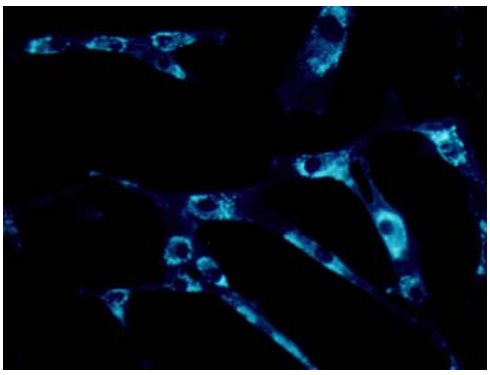

50µg/ml LDL + 10µg/ml progesterone

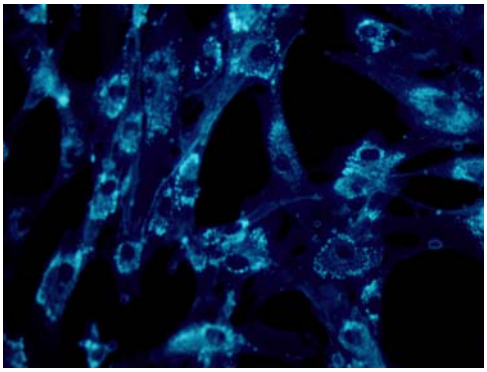

50µg/ml LDL + 10µg/ml progesterone
50µM NB-DNJ

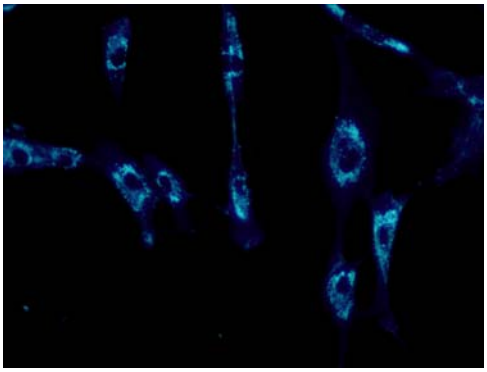

50µg/ml LDL + 10µg/ml progesterone
+ 100µM NB-DNJ

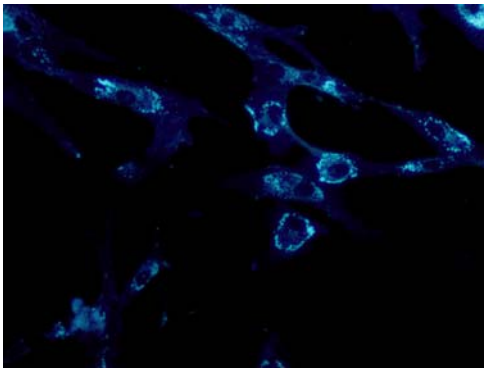

50µg/ml LDL + 10µg/ml progesterone
+ 150µM NB-DNJ

Fig. 3.15 Effect of NB-DNJ on intracellular trafficking of cholesterol in NPC-like human fibroblast cells. Human fibroblast cells were incubated in complete DMEM medium with NB-DNJ (50µM, 100µM, 150µM) or without NB-DNJ, respectively, for 48 hour. The medium was replaced by medium with NB-DNJ (50µM, 100µM, 150µM) or without NB-DNJ, supplementary with 50µg/ml LDL and 10µg/ml progesterone. The cells were incubated for a further 24 hour. The cells were labeled with 50µg/ml filipin at 37 ^{o}C for 30 min. Filipin staining was observed under fluorescence microscope according to the procedure described in Materials and Methods.

Chapter 4. DISCUSSION

4.1. Isolation of lipid rafts

Accumulating evidence suggests that plasma membrane contains lipid raft microdomains which are enriched in cholesterol and sphingolipids. However, much of the evidence comes from model membrane study as it is difficult to detect rafts in cells. This may be due to the following reasons: Firstly, rafts may be too small to be seen in the microscope. Secondly, rafts marker may only have a moderate affinity for rafts and the concentration of these markers in raft domains is not significantly higher than that in non-raft domains. Thirdly, rafts may not exist constitutively but only occur after the clustering of components that have an affinity for raft domains (Brown and London, 2000). These explanations are supported by several recent findings. For example, raft markers, GPI-anchored proteins, were observed to appear uniformly distributed in the plasma membrane (Maxfield and Mayor, 1997). Other markers of rafts, gangliosides, cluster in cell membrane no more than a few molecules (Rock, et al., 1990). However, the distribution of these markers can be changed significantly by clustering with antibodies or other agents. The affinity of these independently clustered molecules suggests that they are all present in rafts (Brown and London, 1998).

There are several outstanding questions on lipid rafts up to today. The size of rafts is still poorly understood. It was reported that gangliosides and a GPI-anchored protein were transiently confined to domains of about 200–300nm (Jacobson and Dietrich, 1999).

Another group found cholesterol dependent clustering into domains which are less than 70nm and are not detectable under microscope (Varma and Mayor, 1998). Another question is about the membrane distribution of rafts. The important component of rafts, GSLs are largely restricted to the outer leaflets of the cell membrane and the behavior of rafts in the cytoplasmic leaflets of the bilayer is still not clear. It is suggested that rafts are present in the inner leaflet and that rafts in the two leaflets are coupled (Harderet, al., 1998). However, how these rafts might be coupled with outer leaflet rafts is very poorly understood. There are some evidences for monolayer coupling of GSL-rich domains in model membranes (Schmidt, et al., 1978). The correlation between the like phases in the two leaflets of model membranes containing two phospholipid species is also shown (Korlach, et al., 1999). In addition, some recent findings showed that plasma membrane phospholipids are more highly saturated than those in intracellular membranes and thus may form rafts in the presence of cholesterol (Fridriksson, et al., 1999). All these observations suggest the possibility of rafts formation in the GSL-poor cytoplasmic membrane leaflet. However, raft behavior in the inner leaflets still needs further investigation.

Detergent extraction is the most commonly used method to study rafts. However, it is argued that DRMs and the proteins associated with DRMs might be artifacts and induced by detergent treatment. Detergent might preferentially extract phospholipids from homogeneous membrane bilayers, leading the remaining insoluble lipids to aggregate. Also detergent extraction might overestimate the amount of lipid or protein in rafts. These lipids or proteins are actually not in raft domains but are driven to partition into

DRMs during detergent extraction. However, there are evidences supporting the reliability of detergent extraction. It was found that DRMs were only formed when L_o phase domains were present in model membrane and detergent did not create insoluble domains when L_o phase domains were absent. Furthermore when non-DRM containing liposomes which contain ^{3}[H] SM were mixed with unlabeled DRM-containing liposomes, all the ^{3}[H] SM in the mixture was triton soluble and did not jump into DRMs during extraction (Schroeder, et al., 1997). All these results strongly proved that detergent does not induce artifacts in the organization of DRM lipids.

In this study, I have isolated the lipid rafts as DRMs by using Triton extraction from the crude membrane fractions of human fibroblast cells. This is based on the insolubility of DRMs in Triton X-100 at 4^{o}C. Then the raft containing fractions were isolated on a 5%, 30%, 40% sucrose step-gradient centrifuge, which is based on the ability of DRMs to float in the density gradient. The raft containing fractions were traced by flotillin-1 and caveolin-1 proteins. Caveolin-1, along with Caveolin-2 and caveolin-3, has been identified as the components of caveolae and is generally regarded as a marker protein of lipid rafts. Flotillin-1 is also identified to localize at the caveolae and regarded as a marker of lipid rafts. The result shows that both caveolin-1 and flotillin-1 peak at light fractions of the gradient [Fig. 3.6]. Caveolin-1 has an additional peak at the bottom of the gradient. This might be due to the whole cells which are accumulated at the heavy fractions during the centrifuge. Another explanation is that caveolin-1 is also present in some non- raft fractions. However, based on the distributions of caveolin-1 and flotillin-1, lipid rafts are confirmed to localize at the light fractions of the gradient. This is consistent

with previous findings that lipid rafts could be isolated as DRMs in the light fractions of density gradient (Hering, et al., 2003). These results show that lipid rafts exist in human fibroblast cells used in this study.

4.2. Effect of NB-DNJ on GSL biosynthesis

GSL are ubiquitous component of the cell membranes and are suggested to play an important role in various biological functions (Hakomori, 1990). The biosynthesis and catabolism of GSLs are tightly controlled. GSL biosynthesis involves the action of a series of enzymes and a key enzyme in the GSL biosynthesis pathway is the Cer specific glucosyltransferase, which catalyzes the first step in GSL biosynthesis (Sandhoff and Van, 1993). As a result, the inhibition of Cer specific glucosyltransferase will result in the depletion of all GSL species. The mutation experiment showed that cells lacking glucosyltransferase did not compromise cell growth and morphology of cells, which suggested that GSLs did not serve a housekeeping function at single cell level (Ishikawa, et al., 1994). However, the precise functions of GSLs still need further investigation both *in vitro* and *in vivo*.

To investigate the function of GSLs in intact organisms, the glucosyltransferase could be inactivated by gene disruption. It is reported that defects in GSL biosynthesis resulted in the disruption of early mammalian development (Sandhoff, et al., 1996). However, the degree to which GSL could be depleted without causing any pathology is still unknown. An alternative approach to manipulate GSL is using specific glucosyltransferase

inhibitors. Cer-specific glucosyltransferase is apparently a preferable target since it inhibits the first step of GSL biosynthesis.

There are two major classes of GSL biosynthesis inhibitors targeting the Cer-specific glucosyltransferase. One is Cer analogues which prevent the glucosylation of Cer by their property of Cer mimicry, such as PDMP (Inokuchi, et al., 1987). Another group of inhibitors are N-alkylated imino sugars, such as NB-DNJ (Platt, et al., 1993). The alkyl chain might play a role in the inhibitory effects here. Alkylated imino sugars have a significant advantage over PDMP and related compound. They have minimal cytotoxicity *in vitro* and are well tolerated *in vivo* (Fischer, et al., 1995). By contrast, the highly hydrophobic property of PDMP might bring toxicity both *in vitro* and *in vivo*. In one study, the effect of D-PDMP and NB-DNJ were investigated in embryonic carcinoma stem cells. It was observed that D-PDMP resulted in reduction of cellular proliferation in embryonal carcinoma stem cells while NB-DNJ had no significant effect on cell growth rate (Liour, et al., 2002). Based on these facts, NB-DNJ could be used as an inhibitor for the Cer-specific glucosyltransferase to manipulate cellular GSL level.

In this study, NB-DNJ was employed to deplete GSL in human fibroblast cells. To evaluate the effect of NB-DNJ on GSL biosynthesis, human fibroblast cells were treated with different doses of NB-DNJ for 72 hour. Compared with other studies using NB-DNJ, relatively low doses of NB-DNJ (50μM, 100μM, 150μM) were used here to minimize the possible side effects. The total lipids were extracted by a standard protocol and the cellular GSL profiles were examined by the HPTLC assay [Fig. 3.1]. The GSLs were

visualized by orcinol-H_2SO_4 reagent and the densities of GSL spots were quantitated [Fig. 3.2]. The results show that GM3 is the most abundant species of GSLs in human fibroblast cells. Other species of GSLs are not detectable by HPTLC which might be due to the limited sensitivity of HPTLC and the low level of these GSLs in human fibroblast cells. The GM3 level was significantly decreased by 70% by treatment with 50μM NB-DNJ. And the inhibition level increased to 80% when the NB-DNJ dose increased to 150μM. These data show that NB-DNJ exhibits a significant inhibition effect on the cellular level of GM3 and this inhibition is dose-dependent. Toxicity of NB-DNJ is also examined by using MTT assay. Results show that NB-DNJ, even at the highest dose of 150μM, does not have any significant effect on cell viability. Taken together, NB-DNJ treatment is potent in the inhibition of GSL biosynthesis and safe to human fibroblast cells.

GM3 belongs to the ganglioside family, which is a large group of sialylated GSLs. Gangliosides are distributed in the outer leaflet of plasma membrane, which is suggested to be enriched in lipid rafts. There are accumulating evidences indicating an important role of gangliosides in raft formation and function. Ganglioside *de novo* biosynthesis starts with the formation of Cer, which is the same with other GSLs. Glc-Cer is then glycosylated to Lac-Cer. Lac-Cer is in turn sialosylated to GM3, GM3 to GD3, GD3 to GT3. GM3, GD3 and GT3 are the starting points for the a-series, b-series and c-series gangliosides respectively. Along each series, non-specific *N*-acetyl-galactosaminyltransferase, galactosyl-transferase and SAT IV introduce a residue of *N*-acetylgalactosamine, galactose, and sialic acid, subsequently, yielding more complex

gangliosides (Huwiler, et al., 2000). Thus the biosynthesis of GM3 is the basis of ganglioside biosynthesis. Along with the fact that NB-DNJ inhibits the very early step of GSL biosynthesis, it is concluded that the decrease of GM3 level is likely to reflect the decrease of the cellular ganglioside and GSL level.

To further investigate the inhibitory effect of NB-DNJ on GSL biosynthesis, the GSL expression at the cell surface was examined. It was predicted that the GM1 level at the cell surface would also be inhibited in the presence of NB-DNJ. The GM1 level was therefore examined by taking advantage of the specific binding of CTxB with GM1. The binding behavior of CTxB was first examined at different temperatures. Human fibroblast cells were stained with Alexa Fluor conjugated CTxB and then incubated at either 0 ^{o}C or 37 ^{o}C for a certain period. The cellular distribution of fluorescent CTxB was examined by fluorescence microscope. The results obtained show that at 0 ^{o}C CTxB only binds to the cell surface GM1 and is not internalized, while at 37 ^{o}C CTxB is internalized after binding to the GM1 receptor [Fig. 3.3]. This result suggests that the cell surface GM1 level will be proportional to the level of CTxB fluorescence at 0 ^{o}C and thus the following binding assay was conducted at 0 ^{o}C. To evaluate whether NB-DNJ inhibits the cell surface GM1 expression, human fibroblast cells were treated with different doses of NB-DNJ (50μM, 100μM, 150μM). The cells were then stained with Alexa Fluor conjugated CTxB. Fluorescence conjugated CTxB binding to cell surface GM1 was detected by using flow cytometry [Fig. 3.4]. The results show that, in the presence of NB-DNJ, CTxB binding to the cell surface GM1 is decreased by up to approximately 60%, indicating a substantial decrease of cell surface GM1 [Fig. 3.5]. Clearly, the inhibition is

NB-DNJ dose-dependent. By taking advantage of the higher sensitivity of flow cytometry than HPTLC, the decrease of cell surface GM1 in the presence of NB-DNJ was observed. These results provide further evidence for the inhibition of GSL biosynthesis by NB-DNJ.

Based on above findings, NB-DNJ treatment efficiently depletes cellular GSLs without apparent side effect on cell viabilities. It becomes possible to investigate the roles of GSLs in raft formation and function by using NB-DNJ. Although it is possible that the depletion of GSLs might be more significant by increasing the dose of NB-DNJ, The concentration used (50μM, 100μM, 150μM) already has a significant inhibition effect, which will be the NB-DNJ concentrations used in the following study.

4.3. Effect of NB-DNJ on raft formation

Because of their tightly packing ability, GSLs are able to interact preferentially with themselves and with SM and cholesterol in a phospholipids environment. Thus GSLs are suggested to be essential for raft formation. A generally accepted model for the organization of rafts suggests that sphingolipids self-associate through weak interactions between the carbohydrate heads of the GSLs and the interaction of GSLs is essential for raft formation. The GSL head groups occupy larger excluded areas in the exoplasmic leaflet than do their highly saturated lipid hydrocarbon chains (Simons and Ikonen, 1997). This model is well supported by studies in model membranes. Particularly, gangliosides GM1 and GM3 were found to be concentrated in caveolae which is suggested to be a type of lipid rafts (Parton, 1994). Furthermore, GM1 was reported to be enriched in different

domains than GM3 does on the same cell (Gomez-Mouton, et al., 2000). Pulse electron paramagnetic resonance spin-labeling method and single-molecule optical techniques have also been applied to investigate the GSL role in rafts. It was found that the size of the confining domain for a GPI-anchored protein is reduced when cells were treated with inhibitors of GSL synthesis, suggesting that GSLs contribute to the formation of rafts (Sheets, et al., 1997).

However, since GSLs are known to be poor in the cytosolic leaflet of cell membranes, this model meets difficulties to explain the raft behavior in the inner leaflet of cell membranes. A second model for raft formation has been proposed. This model postulates that interactions between lipid acyl chains play a key role in raft formation. Particularly, the high Tm of sphingolipids is likely to promote phase separation and formation of raft domains in the presence of high amounts of cholesterol (Brown and London, 1998). Some studies have shown that a long, saturated acyl chain structure can be more important for determining the association of a lipid with Lo domains than the specific structure of its polar head group. For example, phosphatidylethanolamine (PE) was found to have a higher Tm than a PC molecule with an identical acyl chain structure (Koynova, et al., 1994), and was enriched in the inner leaflet. Thus it may play a role in the raft formation in the inner leaflet. An alternate possibility is that other high Tm lipids, such as Cer, may be important for raft formation in inner leaflets.

The role of GSLs in rafts has also been investigated by examining the effect of changing GSL level on functional raft formation. Some researchers found that gangliosides

inhibited the crosslinking of GPI-anchored proteins and increased their detergent solubility. They explained that gangliosides might displace GPI-anchored proteins from rafts by disrupting the interaction between the GPI anchors and surrounding lipids thus the GPI-anchored proteins would be released from rafts. These results suggested that GSLs play a role in raft formation (Mikael, et al., 1999). In another study, GSL synthesis inhibitor, D-PDMP was used to deplete cellular GSLs in lymphocytes. It was observed that the expression state of GPI-anchored proteins was affected by the reduction of GSL levels and the reduction of GSLs in membrane modulated signaling through GPI-anchored proteins. Furthermore, it was also identified that GSL and cholesterol depletion had opposite effects on GPI-anchored proteins in lipid rafts, which suggested a specific role of GSLs in raft formation and function (Masakazu, et al., 2003). A similar study using D-PDMP to deplete GSLs showed that after depletion of GlcCer, LacCer and GM3 from Lewis lung carcinoma cells, most of the Src proteins in low density DRMs were eliminated and shifted to the high density fractions, indicating that GSLs were essential for association of Src kinases with rafts. All these results suggest that GSLs are essential for functional raft formation (Inokuchi, et al., 2000).

However, the group of Brown reported that GSLs might not be essential for raft formation on the basis of their study in melanoma cells (Ostermeyer, et al., 1999). By comparing the DRMs isolated from normal cell and its GSL-deficient derivative, they found that two cell lines had similar DRM protein profiles, while the yield of DRM proteins was 2-fold higher in the normal cells than the mutant cells. They explained that it might be due to cytoskeletal differences. DRMs from the two cell lines had similar

fluidity. Cholesterol was depleted from both cell lines with the same kinetics and to the same extent. Both GPI-anchored proteins and cholesterol showed the same distribution between DRMs and the detergent-soluble fraction after cholesterol depletion in both cell lines. A GPI-anchored protein was delivered to the cell surface at similar rates in the two cell lines, even after cholesterol depletion. They concluded that GSL are not essential for raft formation and function. This finding is contradictory to the findings in other cell lines, which might reflect the differences of raft composition and GSLs' behaviors in different cell lines. It should also be pointed out that the detergent extraction from the cell lysate might underestimate the differences of DRM protein profiles thus it might not precisely reflect the effect of GSL defect on functional raft formation. Furthermore, the different yields of DRM proteins could not be simply explained by cytoskeletal differences. It might be due to the effect of GSL defect on raft formation.

In this study, I employed a technique with the combination of $DiIC_{18}$ staining and confocal microscope. $DiIC_{18}$ is a member of long chain dialkylcarbocyanines. $DiIC_{18}$ labeling does not appreciably affect cell viability, development or basic physiological properties. $DiIC_{18}$ is known to preferentially partition into more-ordered gel phase domains in model membranes (Spink, et al., 1990). It was also reported that a large fraction of $DiIC_{18}$ partitioned into the raft domains of membranes (Sun, et al., 2003). By the aid of this property of $DiIC_{18}$, raft domains could be visualized under confocal microscope in intact cells. Furthermore, DiIC18 staining also provides a chance to visualize raft domains after detergent extraction. After cells are extracted by detergent *in situ*, $DiIC_{18}$ fluorescence remains associated with the insoluble raft domains thus could be

observed under confocal microscope. This approach is advantageous over the detergent extraction method. In this approach, raft domains remain relatively "intacted" and the fluorescent $DiIC_{18}$ incorporated into raft domains might reflect the original localization and organization of rafts in cell membranes. It also becomes possible to quantify the level of raft domains by measuring the $DiIC_{18}$ fluorescence intensity.

This approach has been employed by Maxfield's group to investigate the effect of cholesterol depletion on raft formation. It was observed that in several cell lines, $DiIC_{16,}$ an analog of $DiIC_{18,}$ effectively incorporated into ordered domains of the plasma membranes and remained associated with the cells after cold detergent extraction. Furthermore, they found that when the cellular cholesterol, which was thought to be an important component of rafts, was depleted by a cholesterol biosynthesis inhibitor, $DiIC_{16}$ was also largely removed from cell membranes, suggesting that the rafts in cell membrane was decreased by cholesterol depletion (Hao, et al., 2000).

In this study, to investigate the role of GSLs in raft formation, we treated human fibroblast cells with 50μM NB-DNJ. The cells were then labeled with 10μM fluorescence conjugated $DiIC_{18}$ and observed under confocal microscope. It was found that $DiIC_{18}$ incorporated into the plasma membranes of both control cells and the NB-DNJ treated cells [Fig. 3.7]. $DiIC_{18}$ seemed to be equally distributed in the plasma membranes, indicating that raft domains may have an even distribution in such membranes. The cells were subsequently extracted with 1% Triton X-100 on ice for 20 min. In both the control cells and the NB-DNJ treated cells, $DiIC_{18}$ remained associated with plasma membranes

although the fluorescence intensity decreased. Furthermore we quantified the level of raft domains by manually outlining each cell and taking the average fluorescence intensity associated with the cells. The ratio of the average fluorescence intensity obtained from the detergent extracted cells to that of the intacted cells was used to determine the percentage of the ordered raft domains. It was found that in the presence of 50μM NB-DNJ, the percentage of ordered raft domains was decreased 20% more than that of the intacted cells [Fig. 3.8]. This decrease in raft formation is apparently due to the decrease in GM3 and other GSL species, such as GM1, after NB-DNJ treatment. It thus demonstrated that GSLs, at least certain GSL species, were essential for raft formation in human fibroblast cells and the depletion of these GSLs might affect the formation of rafts in the plasma membranes of the cells. By comparing the results obtained in this study with the data from Maxfield's group, it can be found that the percentage of raft domains in human fibroblast cells is lower than that in other several cell lines examined by them. This might reflect that the raft in human fibroblast cells are not as abundant as in some other cell lines, suggesting that raft may have different abundance in different cells. Nevertheless, the results obtained here are consistent with their finding that the removal of raft components may lead to disruption of the raft structures.

4.4. Effect of NB-DNJ on raft-dependent endocytosis

Endocytosis mediated by caveolae and lipid rafts has been described as the major endocytosis pathway other than the classic clathrin-dependent endocytosis pathway. Caveolae are cholesterol- and GSL- rich smooth invaginations of the plasma membrane

whose formation is associated with caveolin-1 and caveolae constitute a type of biochemically defined lipid rafts (Nabi and Le, 2003). As described in Introduction, caveolin might be not essential for the formation of caveolae. Even in the absence of caveolin, the internalization of rafts may invoke the invagination and budding of a vesicular structure enriched in cholesterol and GSLs. It is proposed that caveolae and rafts may mediate a common endocytic pathway, caveolae/raft-dependent endocytosis.

The best studied particles internalized by caveolae/raft dependent endocytosis are SV40 virus and CTxB. CTxB binds the ganglioside GM1 at the cell surface associated with the lipid rafts (Spangler, 1992). Then CTxB is delivered to a caveolin-1–positive endocytic compartment or caveosome (Parton, et al., 1994; Pelkmans, et al., 2001; Nichols, 2002). Thereafter these particles may enter intracellular targeting routes. In this study, CTxB was employed as a marker to investigate the caveolae/raft dependent endocytosis.

It was reported that in the presence of filipin, the internalization of surface bound CTxB in CaCo-2 cells was inhibited. This inhibition in turn resulted in the blocking of subsequent steps in the intracellular processing of the toxin. These effects of filipin may be attributed to its ability to disrupt the cholesterol-rich raft on the cell surface. In contrast, when cells were exposed to chlorpromazine, which was known as an inhibitor of clathrin coated pits endocytosis, only a slight decrease of toxin binding and uptake were observed. In addition, the combination of chlorpromazine and filipin resulted in nearly complete inhibition of CTxB internalization. These findings suggest that the majority of CTxB was taken up through caveolae/raft-dependent endocytosis although a small

fraction of CTxB could be taken up by clathrin coated pits. Further study showed that CTxB entering cells via clathrin coated pits is unable to activate adenylyl cyclase. (Pacuszka and Fishman., 1992).

It is proposed, as a core component of rafts, the depletion of GSLs should have a similar influence as filipin on the raft-dependent CTxB endocytosis. To investigate the effect of GSL depletion on the raft dependent endocytosis of CTxB, human fibroblast cells were incubated in the presence of different doses of NB-DNJ. Then the cells were labeled with 7.5μM fluorescence conjugated CTxB at 37^{o}C for 5 min [Fig. 3.9], 10 min [Fig. 3.10] and 15 min [Fig. 3.11]. According to the previous study CTxB would be internalized at 37 ^{o}C, thus the fluorescence intensity of CTxB reflects the level of CTxB endocytosis. The cells were examined under fluorescence microscope and the images were quantified by manually outlining each cell and taking the average fluorescence intensity associated with the cells. It was found that in the presence of NB-DNJ the endocytosis of CTxB was significantly decreased in a dose-dependent manner at each of the three time point. In the presence of 50μM of NB-DNJ, the CTxB endocytosis was decreased by 40%. When the NB-DNJ concentration was increased to 150μM, the CTxB endocytosis was decreased by up to 60% [Fig. 3.12]. This inhibition effect of NB-DNJ on CTxB endocytosis might be caused by two possibilities. Firstly, the inhibition of CTxB endocytosis might be due to the decrease of raft structures on the cell surface and the raft-derived transport vesicles which might be necessary for the CTxB transport. Secondly, GSLs might have a specific role in the endocytosis function of lipid rafts. Removing of GSLs not only results in the decrease of rafts structure, but also attenuates the ability of raft in uptaking CTxB.

The second hypothetical explanation is supported by some other findings. It was reported that CTxB associated with GM1 in lipid rafts at the plasma membrane and remained bound to GM1 until arrival in the ER. CTxB was also found to bind to the ER membrane and a significant fraction of the ER form of CTxB was associated with lipid rafts. Furthermore, binding to the ganglioside at the plasma membrane is not sufficient for ER transport. The ganglioside also needs to be associated with lipid rafts. It was suggested that CTxB transport is dependent on gangliosides that associate stably with lipid rafts at least for the transport step from the plasma membrane to the Golgi, indicating a specific role of gangliosides in the raft endocytosis function (Fujinaga, et al., 2003).

In conclusion, the results found in this study show that the depletion of GSL leads to the inhibition of raft dependent endocytosis of CTxB. This is similar with the effect of filipin which might also disrupt lipid rafts. In other words, removal of cellular GSLs may affect the function of lipid rafts.

4.5. Effect of NB-DNJ on intracellular cholesterol trafficking

NPC disease has long been described as a defect in intracellular cholesterol trafficking, in which cholesterol is accumulated in endocytic organelles such as the LE and LY, at the cellular level (Pentchev, et al., 1995). However, recent studies revealed that the level of GSLs, including GM2, was also increased in NPC fibroblasts (Yano, et al., 1996). Thus NPC disease is not only a cholesterol storage disease but also a sphingolipid storage

disease. Furthermore Pagano's group reported that cholesterol homeostasis was perturbed in multiple SLSDs, secondary to sphingolipid accumulation, and cholesterol played a major role in regulating the traffic of sphingolipids along the endocytic pathway (Watanabe, et al., 1998). On the other hand, it was reported that mice neurons in double-deficient of NPC1 and the GSL synthetic enzyme exhibited both lack of GM2 accumulation and dramatic reduction in free cholesterol thus the cholesterol accumulation in NPC1 deficient neurons appeared to be ganglioside dependent. Based on above data it is suggested that there might be a link between cholesterol and GSL homeostasis. Meanwhile, the question was raised: is GSL accumulation secondary to cholesterol accumulation or on the reverse? Since both cholesterol and GSLs are important component for lipid rafts, a model for lipid rafts in mediating cholesterol homeostasis and the GSL homeostasis has been proposed. This model suggests that in lipid storage diseases involving raft lipids, the accumulation of one raft lipid class in the LE and LY would slowly lead to trapping of other raft lipids in the LE and LY (Simons and Gruenberg, 2000).

To elucidate the relationship between cholesterol and GSL homeostasis and test the proposed role of lipid rafts in mediating raft lipids trafficking, it is helpful to examine the intracellular trafficking of cholesterol while GSL level is altered. According to the data shown previously, NB-DNJ efficiently depletes cellular GSLs, it is likely that cholesterol trafficking might also be altered by NB-DNJ treatment. Furthermore, since cholesterol is accumulated in the LE and LY in NPC cells, it is worthwhile to examine, in the presence of NB-DNJ, whether the cholesterol accumulation in NPC-like cells will be altered. As

mentioned before, progesterone is known to induce extensive cholesterol accumulation in the LE and LY in normal cells and the intracellular accumulation of cholesterol in progesterone treated cells is cytochemically indistinguishable from the cholesterol accumulation in the LE and LY in NPC cells (Blanchette-Mackie, et al., 1988). Progesterone was thus employed to induce cholesterol accumulation in the LE and LY which mimic the NPC cells.

Notably it has been reported that after administration of NB-DNJ to the npc mouse, clinical onset and neuropathologic changes were delayed, and life expectancy of the npc mouse was extended by 20–25%. The npc feline model showed a similar response to this therapy (Zervas, et al., 2001). These observations supported the role of GSLs in the neuropathology of NPC and NB-DNJ was suggested to attenuate the NPC pathology. It is worthwhile to investigate whether this therapeutic effect of NB-DNJ is due to the relief of cholesterol accumulation in LE and LY at the cellular level.

In this study, the ability of progesterone to induce cholesterol accumulation in the LE and LY was first confirmed. To enhance the level of cellular cholesterol the cells were loaded with excessive LDL. Then the cells were treated with different doses of progesterone (5μg/ml, 10μg/ml, and 20μg/ml) and were subsequently stained with 50μg/ml filipin at 37 ^{o}C for 30 min. Filipin staining was observed under fluorescence microscope according to the procedure in Materials and Methods. The results show that progesterone induced intense filipin-cholesterol staining in perinuclear vacuoles which are the LE and LY [Fig. 3.13]. Thus progesterone treatment could be used to mimic the NPC like defect

conditions. It was further investigated whether cholesterol intracellular trafficking will be altered in the presence of NB-DNJ. Firstly, normal human fibroblast cells were treated with NB-DNJ (50μM, 100μM and 150μM), cholesterol trafficking was then examined by filipin staining. The results show that, in both presence and absence of NB-DNJ, the cellular cholesterol accumulation levels are similar, indicating that NB-DNJ does not alter the cholesterol trafficking in normal cells [Fig. 3.14]. Secondly, after pretreated with NB-DNJ, the cells were treated with progesterone. The results show that both in presence and absence of NB-DNJ, progesterone induced intense cholesterol accumulation in the LE and LY, suggesting that NB-DNJ does not attenuate the cholesterol jamming [Fig. 3.15].

Taken together, the results suggest that the alteration of GSL level by NB-DNJ does not significantly affect cholesterol trafficking in both normal cells and NPC defect-like cells. Recently another group reported that inhibition of GSL synthesis in NPC cells with NB-DNJ led to marked decreases in GSL but only small decreases in cholesterol accumulation levels. However phenotypes associated with NPC, such as Annexin 2 mislocation, decreased uptake of fluid phase markers and altered LacCer trafficking were all reversed by inhibition of GSL synthesis (Vruchte, et al., 2004).

Based on these findings, it can be suggest that the cholesterol accumulation in NPC disease and other NPC phenotypes, such as Annexin 2 mislocation, decreased uptake of fluid phase markers and altered LacCer trafficking, might be regulated by different mechanisms. Furthermore, the reduction of GSL level alone appeared not sufficient to

alter the cholesterol trafficking. Although NB-DNJ treatment appeared to be effective to attenuate the pathology in npc defect mice (Zervas, et al., 2001), it might be the collective results of GSL depletion and other effects of NB-DNJ on factors mediating cholesterol intracellular trafficking. Such mechanisms mediating cholesterol and GSL homeostasis clearly need further investigations to elucidate.

5. REFERENCE

Almeida, P. F. F., Vaz, W. L. C., and Thompson, T. E. (1992) Lateral diffusion in the liquid-phases of dimyristoylphosphatidylcholine cholesterol lipid bilayers: a free volume analysis. *Biochem.* 31, 6739–6747

Anne A. Wolf, Yukako Fujinaga, and Wayne I. Lencer (2002) Uncoupling of the cholera toxin-G(M1) ganglioside receptor complex from endocytosis, retrograde Golgi trafficking, and downstream signal transduction by depletion of membrane cholesterol. *J. Biol. Chem.* 277, 16249–16256

Anne G. Ostermeyer, Brian T. Beckrich, Kimberly A. Ivarson, Kathleen E. Grove, and Deborah A. Brown (1999) Brown: Glycosphingolipids are not essential for formation of detergent-resistant membrane rafts in melanoma cells. *J. Biol. Chem.* 274, 34459-34466

Anthony H. Futerman and Gerrit Van Meer (2004) The cell biology of lysosomal storage disorders. *Nat. Rev. Mol. Cell Biol.* 5, 554-565

Arni, S., Keilbaugh, S. A., Ostermeyer, A. G., and Brown, D. A. (1998) Association of the neuronal protein GAP-43 with detergent-resistant membranes requires two palmitoylated cysteine residues. *J. Biol. Chem.* 273, 28478–28485

Ayanthi A. Richards, Rainer Pepperkok and Robert G. Parton (2002) Inhibitors of COP-mediated transport and cholera toxin action inhibit simian virus 40 infection. *Mol. Biol. Cell* 13, 1750–1764

B.D. Spangler (1992) Structure and function of cholera toxin and the related Escherichia coli heat-labile enterotoxin. *Microbiol. Rev.* 56, 622–647

Ben Nichols (2003) Caveosomes and endocytosis of lipid rafts. *J. Cell Sci.* 116, 4707-4714

Benmerah, A., Bayrou, M., Cerf Bensussan, N. and Dautry Varsat, A.(1999). Inhibition of clathrin-coated pit assembly by an Eps15 mutant. *J. Cell Sci.* 112, 1303-1311.

Blanchette-Mackie, J. E., Dwyer, N. K., Amende, L. M., Kruth, H. S., Butler, J. D., Sokol, J., Comly, M. E., Vanier, M. T., August, J. T., Bradie, R. O. and Pentchev, P. G (1988) Type-C Niemann-Pick disease: low density lipoprotein uptake is associated with premature cholesterol accumulation in the Golgi complex and excessive cholesterol storage in lysosomes. *Proc. Nat. Acad. Sci. USA* 85, 8022-8026

Brown DA, London E. (1997) Structure of detergent-resistant membrane domains: Does phase separation occur in biological membranes? *Biochem. Biophys. Res. Commun.* 240, 1–7

Brown DA, Rose JK. (1992) Sorting of GPI-anchored proteins to glycolipid-enriched membrane subdomains during transport to the apical cell surface. *Cell* 68, 533–44

Brown MS, Goldstein JL. (1997) The SREBP pathway: regulation of cholesterol metabolism by proteolysis of a membrane-bound transcription factor. *Cell* 89, 331–340

Brown, DA, London, E. (1998) Functions of lipid rafts in biological membranes. *Annu. Rev. Cell Dev. Biol.* 14, 111-136

Bruckner, K., Labrador, J., Scheiffele, P., Herb, A., Seeburg, P., and Klein, R. (1999) EphrinB ligands recruit GRIP family PDZ adaptor proteins into raft membrane microdomains. *Neuron* 22, 511–524

Butler JD, Blanchette-Mackie EJ, Goldin E., O'Neill RR, Carstea G., Roff CF, Patterson MC, Patel S., Comly ME, Cooney A., Vanier MT, Brady RO and Pentchev PG (1992) Progesterone blocks cholesterol translocation from lysosomes. *J. Biol. Chem.* 267, 23797-23805

Carstea ED, Morris JA, Coleman KG, Loftus SK, Zhang D, Cummings C, Gu J, Rosenfeld MA, Pavan WJ, Krizman DB, Nagle J, Polymeropoulos MH, Sturley SL (1997) Niemann-Pick C1 disease gene: homology to mediators of cholesterol homeostasis. *Science* 277, 228–231

Chang CC, Lee CY, Chang ET, Cruz JC, Levesque MC, Chang TY. (1998) Recombinant acyl-CoA:cholesterol acyltransferase-1 (ACAT-1) purified to essential homogeneity utilizes cholesterol in mixed micelles or in vesicles in a highly cooperative manner. *J. Biol. Chem.* 273, 35132–35141

Chang TY, Chang CC, Cheng D. (1997) Acyl-coenzyme A:cholesterol acyltransferase. *Annu. Rev. Biochem.* 66, 613–638

Chen, H., Fre, S., Slepnev, V. I., Capua, M. R., Takei, K., Butler, M. H., Di Fiore, P. P. and de Camilli. P. (1998) Epsin is an EH-domain-binding protein implicated in clathrin-mediated endocytosis. *Nature* 394, 793-797.

Coste, H., Martel, M.B., and Got, R. (1986) Topology of glucosylceramide synthesis in Golgi membranes from porcine submaxillary glands. *Biochim. Biophys. Acta* 858, 6-12

Cruz JC, Sugii S, Yu C, Chang TY (2000) Role of Niemann–Pick type C1 protein in intracellular trafficking of low density lipoprotein-derived cholesterol. *J. Biol. Chem*. 275, 4013– 4021

D.A. Brown, E. London (1998) Structure and origin of ordered lipid domains in biological membranes. *J. Membrane Biol.* 164, 103–114

Danielle Vruchte, Emy Lloyd-Evans, Robert Jan Veldman, David C. A. Neville, Raymond A. Dwek, Frances M. Platt, Wim J. Blitterswijk and Dan J. Sillence (2004) Accumulation of glycosphingolipids in niemann-pick C disease disrupts endosomal transport. *J. Biol. Chem.* 279, 26167-26175

Deborah A. Brown and Erwin London (2000) Structure and function of sphingolipid and cholesterol-rich membrane rafts. *J. Biol. Chem.* 275, 17221–17224

Dietzen DJ, Hastings WR, Lublin DM. (1995) Caveolin is palmitoylated on multiple cysteine residues: Palmitoylation is not necessary for localization of caveolin to caveolae. *J. Biol. Chem.* 270, 6838–42

DJ Carey and CB Hirschberg (1981) Topography of sialoglycoproteins and sialyltransferases in mouse and rat liver Golgi. *J. Biol. Chem.* 256, 989-993

E. London, DA Brown (2000) Insolubility of lipids in triton X-100: physical origin and relationship to sphingolipid/cholesterol membrane domains (rafts). *Biochim.Biophys. Acta* 1508, 182–195.

Eskelinen, E. L., Tanaka, Y. and Saftig, P. (2003) At the acidic edge: emerging functions for lysosomal membrane proteins. *Trends Cell Biol.* 13, 137–145

Field, K. A., Holowka, D., and Baird, B. (1999) Structural aspects of the association of fcepsilon RI with detergent-resistant membranes. *J. Biol. Chem.* 274, 1753–1758

Ford, M. G., Pearse, B. M., Higgins, M. K., Vallis, Y., Owen, D. J., Gibson, A., Hopkins, C. R., Evans, P. R. and McMahon, H. T. (2001). Simultaneous binding of PtdIns(4,5)P2 and clathrin by AP180 in the nucleation of clathrin lattices on membranes. *Science* 291, 1051-1055

Frances M. Platt, Gabriele Reinkensmeier (1997) Extensive glycosphingolipid depletion in the liver and lymphoid organs of mice treated with N-butyldeoxynojirimycin. *J. Biol. Chem.* 272, 19365-19372

Fridriksson, E.K., Shipkova, P.A., Sheets, E.D., Holowka, D., Baird, B., and McLafferty, F.W. (1999) Quantitative analysis of phospholipids in functionally important membrane domains from RBL-2H3 mast cells using tandem high-resolution mass spectrometry. *Biochemistry* 38, 8056–8063

Fujimoto T. (1996) GPI-anchored proteins, glycosphingolipids, and sphingomyelin are sequestered to caveolae only after crosslinking. *J. Histochem. Cytochem*. 44, 929–41

Futerman AH, Pagano RE (1991) Determination of the intracellular sites and topology of glucosylceramide synthesis in rat liver. *Biochem. J.* 280, 295–302

G. Tettamanti (2004) Ganglioside/glycosphingolipid turnover: new concepts. *Glycoconj. J.* 20, 301–17

H. Watari, EJ Blanchette-Mackie, NK Dwyer, JM Glick, S. Patel, EB Neufeld, ROBrady, PG Pentchev, and JF Strauss (1999) Niemann–Pick C1 protein: obligatory roles for N-terminal domains and lysosomal targeting in cholesterol mobilization. *Proc. Natl. Acad. Sci. USA* 96 (3), 805–810

Hao Pang, Phuong U. Le and Ivan R. Nabi (2004) Ganglioside GM1 levels are a determinant of the extent of caveolae/raft-dependent endocytosis of cholera toxin to the Golgi apparatus. *J. of Cell Sci.* 117, 1421-1430

Heike Hering, Chih-Chun Lin, and Morgan Sheng (2003) Lipid rafts in the maintenance of synapses, dendritic spines, and surface AMPA receptor stability. *The Journal of Neuroscience* 23(8), 3262–3271

Harder, T., Scheiffele, P., Verkade, P., and Simons, K. (1998) Lipid domain structure of the plasma membrane revelaed by patching of membrane components. *J. Cell Biol*. 141, 929–942

Higgins ME, Davies JP, Chen FW (1999) Niemann–Pick C1 is a late endosome-resident protein that transiently associates with lysosomes and the trans-Golgi network. *Mol. Genet. Metab.* 68 (1), 1 –13

Hua X, Nohturfft A, Goldstein JL, Brown MS. (1996) Sterol resistance in CHO cells traced to point mutation in SREBP cleavage-activating protein. *Cell* 87, 415–426

Huwiler A, Kolter T, Pfeilschifter J, Sandhoff K, (2000) Physiology and pathophysiology of sphingolipid metabolism and signaling, *Biochim. Biophy. Acta* 1485, 63–9

Inokuchi JI, Uemura S, Kabayama K, Igarashi Y. (2000) Glycosphingolipid deficiency affects functional microdomain formation in Lewis lung carcinoma cells. *Glycoconj. J.* 17, 239–245

Ipsen, J. H., Karlstrom, G., Mouritsen, O. G., Wennerstrom, H., and Zuckermann, M. J. (1987) Phase. equilibria in the phosphatidylcholine–cholesterol system. *Biochim. Biophys. Acta* 905, 162– 39.

Jeckel, D., Karrenbauer, A., Burger, KNJ, Van Meer, G., and Wieland, F. (1992) Glucosylceramide is synthesized at the cytosolic surface of various Golgi Subfractions. *J. Cell Biol.* 117, 259-267

Journet, A., Chapel, A., Kieffer, S., Roux, F. and Garin, J. (2002) Proteomic analysis of human lysosomes: application to monocytic and breast cancer cells. *Proteomics* 2, 1026–1040

K. Jacobson, C. Dietrich (1999) Looking at lipid rafts. *Trends Cell Biol*. 9, 87-91

K. Simons, D. Toomre (2000) Lipid rafts and signal transduction. *Nat. Rev. Mol. Cell Biol.* 1(1), 31-9.

Karlsson KA. (1970) Sphingolipid long chain bases. *Lipids* 5, 878–91

Keenan TW, Morre DJ, Basu S (1974) Ganglioside biosynthesis. Concentration of glycosphingolipid glycosyltransferases in Golgi apparatus from rat liver. *J. Biol. Chem*. 249, 310–5

Kobayashi T, Beuchat MH, Lindsay M, Frias S, Palmiter RD, Sakuraba H, Parton RG, Gruenberg J (1999) Late endosomal membranes rich in lysobisphosphatidic acid regulate cholesterol transport. *Nat. Cell Biol*. 1, 113–118

Kobayashi T, Beuchat MH, Lindsay M, Frias S, Palmiter RD, Sakuraba H, Parton RG, Gruenberg J. (1999) Late endosomal membranes rich in lysobisphosphatidic acid regulate cholesterol transport. *Nat. Cell Biol*. 1(2), 113–118

Kobayashi T, Stang E, Fang KS, De Moerloose P, Parton RG, Gruenberg J. (1998) A lipid associated with antiphospholipid syndrome regulates endosome structure and function. *Nature* 392, 193– 197

Korlach, J., Schwille, P., Webb, W. W., and Feigenson, G. W. (1999) Characterization of lipid bilayer phases by confocal microscopy and fluorescence correlation spectroscopy. *Proc. Natl. Acad. Sci. USA* 96, 8461–8466

L. Liscum, J.J. Klansek (1998) Niemann–Pick disease type C. *Curr. Opin. Lipid* 9(2), 131– 135

L. Liscum, J.R. Faust (1989) The intracellular transport of low density lipoprotein-derived cholesterol is inhibited in Chinese hamster ovary cells cultured with 3-h-[2-(diethylamino)ethoxy]androst-5-en-17-one. *J. Biol. Chem.* 264, 11796– 11806

Lawrence Rajendran, Kai Simons (2005) Lipid rafts and membrane dynamics. *J. of Cell Sci.* 118, 1099-1102

Lindberg AA, Brown JE, Stromberg N, Westling-Ryd M, Schultz JE, Karlsson KA. (1987) Identification of the carbohydrate receptor for Shiga toxin produced by Shigella dysenteriae type 1. *J Biol. Chem.* 262, 1779–1785

Ling H, Boodhoo A, Hazes B, Cummings MD, Armstrong GD, Brunton JL, Read RJ. (1998) Structure of the shiga-like toxin I B-pentamer complexed with an analogue of its receptor Gb3. *Biochemistry* 37, 1777–1788

Lipsky, NG, Pagano, RE (1985) Intracellular translocation of fluorescent. sphingolipids in cultured fibroblasts. *J. Cell Biol.* 100, 27-34

Liscum L. (2000) Niemann-Pick type C mutations cause lipid traffic jam. *Traffic* 1, 218-25

M. Ge, K.A. Field, R. Aneja, D. Holowka, B. Baird, J.H. Freed, (1999) Electron spin resonance characterization of liquid ordered phase of detergent resistant membranes from RBL-2H3 cells. *Biophys. J.* 77, 925-933

Machleidt, T., Li, W.P., Liu, P., and Anderson, R. G. W. (2000) Multiple domains in caveolin-1 control its intracellular traffic. *J. Cell Biol.* 148, 17–28

Maekawa S, Kumanogoh H, Funatsu N, Takei N, Inoue K, (1997) Identification ofNAP-22 and GAP-43 (neuromodulin) as major protein components in a Triton insoluble low density fraction of rat brain. *Biochim. Biophys. Acta* 1323, 1–5

Majoul IV, Bastiaens PI, Soling HD (1996) Transport of an external Lys-Asp-Glu-Leu (KDEL) protein from the plasma membrane to the endoplasmic reticulum: studies with cholera toxin in Vero cells. *J. Cell Biol*. 133, 777–789

Majoul, I., Sohn, K., Wieland, FT, Pepperkok, R., Pizza, M., Hillemann, J., Soling, HD (1998) KDEL receptor (Erd2p)-mediated retrograde transport of the cholera toxin A subunit from Golgi involves COPI, p23, and the COOH terminus of Erd2p. *J. Cell Biol.* 143, 601–612.

Mandon, E. C., Ehses, I., Rother, J., Van Echten, G. and Sandhoff, K (1992) Subcellular localization and membrane topology of serine palmitoyltransferase, 3-dehydrosphinganine reductase, and sphinganine N-acyltransferase in mouse liver. *J. Biol. Chem.* 267, 11144-11148

March PA, Thrall MA, Brown DE, Mitchell TW, Lowenthal AC, Walkley SU (1997) GABAergic neuroaxonal dystrophy and other cytopathological alterations in feline Niemann–Pick disease type C. *Acta Neuropathol.* 94 (2), 164– 172

Marjorie C. Gondre Lewis, Robert McGlynn, and Steven U. Walkley (2003) Cholesterol Accumulation in NPC1-Deficient Neurons Is Ganglioside Dependent. *Current Biology* 13, 1324–1329

Marks, DL and Pagano, RE (2002) Endocytosis and sorting of glycosphingolipids in sphingolipid storage disease. *Trends Cell Biol.* 12, 605-613

Masakazu Nagafuku, Kazuya Kabayama, Daisuke Oka, Akiko Kato, Shizue Tani-ichi, Yukiko Shimada, Yoshiko Ohno-Iwashita, Sho Yamasaki, Takashi Saito, Kazuya Iwabuchi, Toshiyuki Hamaoka, Jin-ichi Inokuchi, and Atsushi Kosugi (2003) Reduction of glycosphingolipid levels in lipid rafts affects the expression state and function of

glycosylphosphatidylinositol-anchored proteins but does not impair signal transduction via the T cell receptor. *J. Biol. Chem*. 278, 51920–51927

Mateo, C. R., Acuna, A. U. and Brochon, J.C. (1995) Liquid-crystalline phases of cholesterol/lipid bilayers as revealed by the fluorescence of trans-parinaric acid. *Biophys.* 131, 125–136

McConville MJ, Ferguson MAJ. (1993) The structure, biosynthesis and function of glycosylated phosphatidylinositols in the parasitic protozoa and higher eukaryotes. *Biochem. J.* 294, 305–24

Melkonian, K. A., Ostermeyer, A. G., Chen, J. Z., Roth, M. G., and Brown, D. A. (1999) Role of lipid modifications in targeting proteins to detergent-resistant membrane rafts: Many raft proteins are acylated, while few are prenylated. *J. Biol. Chem.* 274, 3910–3917

Merritt EA, Hol WG. (1995) AB5 toxins. *Curr. Opin. Struct. Biol*. 5, 165–171

Middleton, J., Neil, S., Wintle, J., Clarke-Lewis, I., Moore, H., Lam, C., Auer, M., Rot, A. (1997) Transcytosis and surface presentation of IL-8 by venular endothelial cells. *Cell* 91, 385–395

Mikael Simons, Tim Friedrichson, Jorg B. Schulz, Marina Pitto, Massimo Masserini, and Teymuras V. Kurzchalia (1999) Exogenous administration of gangliosides displaces GPI-anchored proteins from lipid microdomains in living cells. *Mol. Biol. of the Cell* 10, 3187–3196

Milligan G, Parenti M, Magee AI. (1995) The dynamic role of palmitoylation in signal transduction. *Trends Biochem. Sci.* 20, 181–187

Mingming Hao, Sushmita Mukherjee, and Frederick R. Maxfield (2001) Cholesterol depletion induces large scale domain segregation in living cell membranes. *Proc. Natl. Acad. Sci. USA* 98, 13072–13077

Moffett, S., Brown, D. A., and Linder, M. E. (2000) Lipid-dependent targeting of G proteins into rafts. *J. Biol. Chem.* 275, 2191–2198

Moldovan, N. I., Heltianu, C., Simionescu, N., and Simionescu, M. (1995) Ultrastructural evidence of differential solubility in Triton X-100 of endothelial vesicles and plasma membrane. *Exp. Cell Res*. 219, 309–313.

Montesano R, Roth J, Robert A, Orci L. (1982) Non-coated membrane invaginations are involved in binding and internalization of cholera and tetanus toxins. *Nature* 296, 651–653

Mosmann T. (1983) Rapid colorimetric assay for cellular growth and survival: application to proliferation and cytotoxicity assays. *J. Immunol. Methods.* 65(1-2), 55-63

Mukherjee, S. and Maxfield, FR (2004) Lipid and cholesterol trafficking in NPC. *Biochim. Biophys. Acta* 1685, 28-37

Nabi and Phuong U. Le (2003) Caveolae/raft-dependent endocytosis. *J. Cell Biol.* 161, 673-677

Neufeld EB, Wastney M, Patel S, Suresh S, Cooney AM, Dwyer NK, Roff CF, Ohno K, Morris JA, Carstea ED, Incardona JP, Strauss JF, Vanier MT, Patterson MC, Brady RO, Pentchev PG, Blanchette-Mackie EJ (1999) The Niemann–Pick C1 protein resides in avesicular compartment linked to retrograde transport of multiple lysosomal cargo. *J. Biol. Chem*. 274, 9627– 9635.

Orlandi, P. A. and Fishman, P. H. (1998) Filipin-dependent inhibition of cholera toxin: evidence for toxin internalization and activation through caveolae-like domains. *J. Cell Biol.* 141, 905-915

P.G. Pentchev (1995) Niemann–Pick Disease type C: cellular cholesterol lipidosis. *McGraw-Hill, New York*, 2625–2639.

P.W. Janes, S.C. Ley, A.I. Magee (2000) Aggregation of lipid rafts accompanies signaling via the T cell antigen receptor. *J. Cell Biol.* 19, 892-901

Pagano RE, Sleight RG. (1985) Defining lipid transport pathways in animal cells. *Science* 229, 1051-1057

Parton RG, Joggerst B, Simons K. (1994) Regulated internalization of caveolae. *J. Cell Biol.* 127, 1199–1215

Parton RG. (1994) Ultrastructural localization of gangliosides; GM1 is concentrated in caveolae. *J. Histochem Cytochem*. 42, 155–66

Parton, R. G., Joggerst, B. and Simons, K. (1994) Regulated internalization of caveolae. *J. Cell Biol.* 127, 1199-1215

Pascher I. (1976) Molecular arrangements in sphingolipids. Conformation and hydrogen bonding of ceramide and their implicationon membrane stability and permeability. *Biochim. Biophy.s Acta* 455, 433–51

Paula Upla , Varpu Marjomaki , Pasi Kankaanpaa, Johanna Ivaska , Timo Hyypia , F. Gisou van der Goot, and Jyrki Heino (2004) Clustering induces a lateral redistribution of α2β1 integrin from membrane rafts to caveolae and subsequent protein kinase C-dependent internalization. *Mol. Biol. Cell* 15, 625-636

Pelkmans L, Puntener D, Helenius A. (2002) Local actin polymerization and dynamin recruitment in SV40-induced internalization of caveolae. *Science* 296, 535–539

Pentchev PG, Comly ME, Kruth HS, Vanier MT, Wenger DA, Patel S, Brady RO. (1985) A defect in cholesterol esterification in Niemann–Pick disease (type C) patients. *Proc. Natl. Acad. Sci. USA* 82, 8247– 8251.

Perschl, A., Lesley, J., English, N., Hyman, R., and Trowbridge, I. S. (1995) Transmembrane domain of CD44 is required for its detergent insolubility in fibroblasts. *J. Cell Sci.* 108, 1033–1041

Pike, L. J. (2004) Lipid rafts: heterogeneity on the high seas. *Biochem. J.* 378, 281–292

Platt, F. M., Neises, G. R., Karlsson, G. B., Dwek, R. A., and Butters, T. D. (1994) Butyldeoxygalactonojirimycin Inhibits Glycolipid biosynthesis but does not affect N-linked oligosaccharide processing. *J. Biol. Chem.* 269, 27108-27114

Platt, F. M., Neises, G. R., Karlsson, G. B., Dwek, R. A., and Butters, T. D. (1994) N-Butyldeoxynojirimycin is a novel inhibotor of glycolipid biosynthesis. *J. Biol. Chem.* 269, 27108-27114

Polyak, M. J., Tailor, S. H., and Deans, J. P. (1998) Identification of a cytoplasmic region of CD20 required for its redistribution to a detergent-insoluble membrane compartment. *J. Immunol*. 161, 3242–3248

Puertollano, R., and Alonso, M. A. (1998) A short peptide motif at the carboxyl terminus is required for incorporation of the integral membrane MAL protein to glycolipid-enriched membranes. *J. Biol. Chem.* 273, 12740–12745

Puri V, Watanabe R, Dominguez M, Sun X, Wheatley CL, Marks DL, Pagano RE. (1999) Cholesterol modulates membrane traffic along the endocytic pathway in sphingolipid storage diseases. *Nat. Cell Biol.* 1, 386–388

Recktenwald, D. J., and McConnell, H. M. (1981) Phase equilibria in binary mixtures of phosphatidylcholine and cholesterol. *Biochem.* 20, 4505–4510

Resh MD. (1994) Myristylation and palmitylation of Src family members: the fats of the matter. *Cell* 76, 411–413

Robbins SM, Quintrell NA, Bishop JM. (1995) Myristoylation and differential palmitoylation of the HCK protein-tyrosine kinases govern their attachment to membranes and association with caveolae. *Mol. Cell. Biol*. 15, 3507–3515

Rosenthal MD. (1987) Fatty acid metabolism of isolated mammalian cells. *Prog. Lipid Res.* 26, 87–124

Patel SC, Suresh S, Kumar U, Hu CY, Cooney A, Blanchette-Mackie EJ, Neufeld EB, Patel RC, Brady RO, Patel YC (1999) Localization of Niemann–Pick C1 protein in astrocytes: implications for neuronal degeneration in Niemann–Pick type C disease. *Proc. Natl. Acad. Sci. USA* 96 (4), 1657– 1662

Sakai J, Rawson RB, Espenshade PJ, Cheng D, Seegmiller AC, Goldstein JL, Brown MS (1998) Molecular identification of the sterol-regulated luminal protease that cleaves SREBPs and controls lipid composition of animal cells. *Mol. Cell* 2, 505–514

Sankaram, M. B., and Thompson, T. E. (1990) Interaction of cholesterol with various glycerophospholipids and sphingomyelin. *Biochem*. 29, 10670–10675

Sargiacomo, M., Sudol, M., Tang, A. and Lisanti, M. P. (1993). Signal transducing molecules and GPI-linked proteins form a caveolin-rich insoluble complex in MDCK cells. *J. Cell Biol*. 122, 789-807

Satoshi B. Sato, Kumiko Ishii, Asami Makino, Kazuhisa Iwabuchi, Akiko Yamaji Hasegawa, Yukiko Senoh, Isao Nagaoka, Hitoshi Sakuraba, and Toshihide Kobayashi (2004) Distribution and transport of cholesterolrich membrane domains monitored by a membraneimpermeant fluorescent polyethylene glycol-derivatized cholesterol. *J. Biol. Chem*. 279, 23790–23796

Scheiffele, P., Roth, M. G., and Simons, K. (1997) Interaction of influenza virus haemagglutinin with sphingolipid cholesterol membrane domains via its transmembrane domain. *EMBO J.* 16, 5501–5508

Schmidt, C. F., Barenholz, Y., Huang, C., and Thompson, T. E. (1978) Monolayer coupling in sphingomyelin bilayer systems. *Nature* 271, 775–777

Schroeder, R., London, E., and Brown, D. A. (1994) Interactions between saturated acyl chains confer detergent resistance on lipids and GPI-anchored proteins: GPI anchored proteins in liposomes and cells show similar behavior. *Proc. Natl. Acad. Sci. USA* 91, 12130–12134

Sheets, E.D., Lee, G.M., Simson, R., Jacobson, K. (1997) Transient confinement of a glycosylphosphatidylinositol-anchored protein in the plasma membrane. *Biochemistry* 36, 12449–12458

Shenoy-Scaria AM, Dietzen DJ, Kwong J, Link DC, Lublin DM. (1994) Cysteine3 of Src family protein tyrosine kinases determines palmitoylation and localization in caveolae. *J. Cell Biol*. 126, 353–64

Silvius JR, Del Guidice D, Lafleur M. (1996) Cholesterol at different bilayer concentrations can promote or antagonize lateral segregation of phospholipids of differing acyl chain length. *Biochemistry* 35, 15198–208

Simons K, Gruenberg J. (2000) Jamming the endosomal system: lipid rafts and lysosomal storage diseases. *Trends Cell Biol.* 10, 459-462

Simons, K. and Toomre, D. (2000) Lipid rafts and signal transduction. *Nature Rev. Mol. Cell Biol*. 1, 31–39

Simons, K., and Ikonen, E. (1997) Functional rafts in cell membranes. *Nature* 387, 569-572

Singer, S. J. and Nicolson, G. L. (1972) The fluid mosaic model of the structure of cell membranes. *Science* 175, 720-731

Smart EJ, Ying YS, Donzell WC, Anderson RGW. (1996) A role for caveolin in transport of cholesterol from endoplasmic reticulum to plasma membrane. *J. Biol. Chem.* 271, 29427–35

Stacie K. Loftus, Jill A. Morris, Eugene D. Carstea, Jessie Z. Gu, Christiano Cummings, Anthony Brown, Jane Ellison, Kousaku Ohno, Melissa A. Rosenfeld (1997) Murine model of Niemann-Pick C disease: mutation in a cholesterol homeostasis gene. *Science* 277, 232–235

T. Kobayashi, F. Gu, J. Gruenberg (1998) Lipids, lipid domains and lipid–protein interactions in endocytic membrane traffic. *Semin. Cell Dev. Biol.* 9(5), 517–526.

T. Pacuszka, R. O. Duffard, R. N. Nishimura, R. O. Brady, and P. H. Fishman (1978) Biosynthesis of bovine thyroid gangliosides. *J. Biol. Chem*. 253, 5839-5846

T. Yano (1996) Accumulation of GM2 ganglioside in Niemann–Pick disease type C fibroblasts. *Proc. Jpn. Acad.* 72, 214– 219

Tadano-Aritomi T, Kubo H, Ireland P, Hikata T, Ishizuka I, (1998) Isolation and characterization of a unique sulfated ganglioside, sulfated GM1a, from rat kidney. *Glycobiology* 8, 341–50

Thompson TE, Tillack TW. (1985) Organization of glycosphingolipids in bilayers and plasma membranes of mammalian cells. *Annu. Rev. Biophys. Biophys. Chem*. 14, 361–86

Tran D, Carpentier JL, Sawano F, Gorden P, Orci L. (1987). Ligands internalized through coated or noncoated invaginations follow a common intracellular pathway. *Proc. Natl. Acad. Sci. USA* 84, 7957–61

Trinchera, M., Fabbri, M. & Ghidoni, R. (1991) Topography of glycosyltransferases involved in the initial glycosylations of gangliosides. *J. Biol. Chem*. 266, 20907–20912

V.D. Bliek, A. M., Redelmeier, T. E., Damke, H., Tisdale, E. J., Meyerowitz, E. M. and Schmid, S. L. (1993). Mutations in human dynamin block an intermediate stage in coated

vesicle formation. *J. Cell Biol.* 122, 553-563.

Van Meer, G. (1989) Lipid traffic in animal cells. *Annu. Rev. Cell Biol.* 5, 247-275

Vist, M. R., and Davis, J. H. (1990) Phase equilibria of cholesterol / dipalmitoylphosphatidylcholine mixtures: 2H nuclear magnetic resonance and differential scanning calorimetry. *Biochem.* 29, 451–464

Wolf AA, Jobling MG, Wimer-Mackin S, Ferguson-Maltzman M, Madara JL, Holmes RK, Lencer WI (1998) Ganglioside structure dictates signal transduction by cholera toxin in polarized epithelia and association with caveolae-like membrane domains. *J. Cell Biol.* 141, 917–927

Y. Lange, J. Ye, M. Rigney, and T. Steck (2000) Cholesterol movement in Niemann-Pick Type C cells and in cells treated with amphiphiles. *J. Biol. Chem*. 275, 17468 - 17475

Y.A. Ioannou (2000) The structure and function of the Niemann–Pick C1 protein. *Mol. Genet. Metab*. 71 (1–2), 175–181

Y.A. Ioannou (2001) Multidrug permeases and subcellular cholesterol transport. *Nat. Rev., Mol. Cell Biol*. 2 (9), 657– 668

Yukako Fujinaga, Anne A. Wolf, Chiara Rodighiero, Heidi Wheeler, Billy Tsai, Larry Allen, Michael G. Jobling , Tom Rapoport , Randall K. Holmes , and Wayne I. Lencer (2003) Gangliosides that associate with lipid rafts mediate transport of cholera and related toxins from the plasma membrane to endoplasmic reticulm. *Mol. Biol. Cell* 14, 4783-4793

Yusuf, H. K. M., Pohlentz, G., and Sandhoff, K. (1983) Ganglioside GM2 as a human tumor antigen (OFA-I-1). *Proc. Natl. Acad. Sci. USA* 80, 7075-7079

Yusuf, H. K. M., Pohlentz, G., Schwarzmann, G., and Sandhoff, K. (1983) Ganglioside biosynthesis in Golgi apparatus of rat liver: stimulation by phosphatidylglycerol and inhibition by tunicamycin. *Eur. J. Biochem*. 134, 47-54

Yu Sun, Mingming Hao, Yi Luo, Chien-ping Liang, David L. Silver, Celina Cheng, Frederick R. Maxfield, and Alan R. Tall (2003) Stearoyl-CoA desaturase inhibits ATP-binding Cassette Transporter A1-mediated cholesterol efflux and modulates membrane domain structure. *J. Biol. Chem.* 278, 5813–5820

Zelenski NG, Rawson RB, Brown MS, Goldstein JL. (1999) Membrane topology of S2P, a protein required for intramembranous cleavage of sterol regulatory element-binding proteins. *J. Biol. Chem.* 274, 21973–21980

Zervas M, Somers KL, Thrall MA, Walkley SU (2001) Critical role for glycosphingolipids in Niemann-Pick disease type C. *Curr. Biol*. 11(16), 1283-1287

Zhang, W., Trible, R. P., and Samelson, L. E. (1998) LAT palmitoylation: its essential role in membrane microdomain targeting and tyrosine phosphorylation during T cell activation. *Immunity* 9, 239–246